Final Report
Contract: NASW-99004
Period: 4 March 1999 - 4 March 2002
Principal Investigator: Daniel R. Weimer

Title of Investigation: "Obtaining reliable predictions of Terrestrial energy coupling from real-time solar wind measurements"

The objective of this project was to use measurements from multiple satellites in the "upstream" solar wind to determine how the temporal and spatial scales affect the ability to make reliable predictions of the Earth's "space weather" from measurements at the L1 orbit. Following this, the next objective was to develop techniques to improve the timing of the predictions, and then, determine how well the ionospheric parameters that are predicted by the solar wind measurements compare to actual measurements.

The primary focus of this investigation was to be the measurements from the ACE spacecraft, with secondary data obtained from Wind, IMP-8, and Geotail. Measurements from all four spacecraft were used extensively in this project. To summarize the main findings, it was found that the interplanetary magnetic field (IMF) measured with four different spacecraft in the solar wind correlated to a surprisingly high degree, but only after making continuously variable adjustments to the timing of the propagation delays between the satellites. These results could be explained as due to variations in the orientation of the plane of constant phase. In other words, the "phase fronts" were tilted with respect to the propagation direction along the Sun-Earth line. The implication for "space weather" predictions is that there is a very high confidence in that the IMF that is measured at the L_1 orbit will be the same that later impacts the Earth's magnetosphere; the only question is exactly when, as the tilting of the phase fronts introduces uncertainties in the timing of up to 30 to 40 minutes. More extensive details about these results are contained in Appendix A, which contains the manuscript titled "*Variable time delays in the propagation of the interplanetary magnetic field.*" This paper has been accepted for publication in *The Journal of Geophysical Research* and currently is "in press".

These findings had been accomplished with the use of measurements from four spacecraft in the solar wind, and subsequently there was a need to be able to determine the orientation of the tilted phase planes in near real time, using only the IMF measurements available from a single spacecraft, such as ACE. It was found that this task could be accomplished with use of the "minimum variance" technique, as described in Appendix B, titled "*Predicting IMF propagation delay times using the minimum variance technique.*" This manuscript will be submitted for publication to JGR very shortly.

There have also been good results in predicting ionospheric parameters from solar wind measurements. Predictions using the ACE data in conjunction with the "Weimer 2001"[1] electric potential model had been shown at the 2000 Space Weather Week hosted by the NOAA Space Environment Laboratory. The objective of this "prediction challenge" was to predict magnetic variations measured on the ground. In the following year the challenge was given to predict ion

[1]Weimer, D. R., An improved model of ionospheric electric potentials including substorm perturbations and application to the GEM November 24, 1996 event, *J. Geophys. Res., 106,* 407, 2001.

drift velocities, or electric fields, measured by the DMSP spacecraft. Again the model results were good, often superior to those from supercomputer MHD simulations. Details about both challenge results were given in earlier progress reports.

The calculations of magnetic perturbations in the first challenge had used the electric potential model in combination with an ad hoc ionospheric conductivity model. This conductivity model had been constructed by a statistical comparison of electric field predictions and actual magnetometer measurements at the desired sites for several other days of the month, and hence were valid only for those sites at that time of year. More recently it had been realized that it would be possible to obtain predictions of magnetic perturbations on the ground by use of a field-aligned current model that was constructed with magnetic Euler potentials[2]. This could be done without the need for any ionospheric conductivity model, and yet obtain better results. The use of this technique, in combination with the minimum variance calculation of IMF phase plane, is demonstrated in Appendix B. While both the electric potential and field-aligned current models were previously developed under other programs, the technique for practicable application of these models to the prediction of geomagnetic effects with the ACE data were developed under this contract. Continued work on this technique, including publication, will be conducted within the context of a newer NASA contract through the Living With a Star program.

In summary, all of the stated project objectives were attained to a high degree of success. The work on the tilted phase planes required a long-duration development of a considerable amount of new and unique computer code, which precluded a large publication list from this project. However, the final publications are expected to be regarded as important, milestone works in the prediction of terrestrial space weather from the real-time solar wind and IMF measurements.

[2]Weimer, D. R.,Maps of field-aligned currents as a function of the interplanetary magnetic field derived from Dynamics Explorer 2 data, *J. Geophys. Res.,106,* 12,889, 2001.

Variable time delays in the propagation of the interplanetary magnetic field

D. R. Weimer[1], D. M. Ober[1], N. C. Maynard[1], W. J. Burke[2], M. R. Collier[3], D. J. McComas[4], N. F. Ness[5], and C. W. Smith[5]

(To be published by the *Journal of Geophysical Research*)

Abstract. Simultaneous measurements of the Interplanetary Magnetic Field (IMF) are obtained at various locations with four spacecraft, ACE, Wind, IMP-8, and Geotail. We have devised a technique whereby the exact propagation delay time between ACE , at the L1 orbit, and each of the other three spacecraft can be derived from these measurements. This propagation delay is determined as a continuously varying function of time; when this measured delay is applied to all three components of the IMF measured by ACE they will match the other satellites' IMF to a degree that is much better than expected. But the actual time delays can vary by nearly an hour in either direction from the expected advection delays, and the lag times have significant changes that can occur on a time scale of a few minutes. These results are interpreted as due to the effects of tilted phase fronts which are changing orientation with time. We have used the delay measurements between multiple satellites to calculate the three-dimensional orientation and temporal variations of the phase front. The best-fit phase front plane usually lies within 4 R_E or less from the four-point measurements, indicating a lag resolution of a minute or less. Computer animations of the time-varying phase fronts are used to illustrate their behavior. Orientations can change on short time scales. Our findings have implications for both basic research and "space weather" predictions. These results give a high confidence that the same IMF that is measured near L1 will most likely impact the Earth's magnetosphere, providing ample justification for use of spacecraft data in halo orbit at L1 for monitoring the upstream solar wind prior to its interacting with the magnetosphere. However, there is strong uncertainty in the timing of the arrival of the detailed IMF structures, and these delays will need to be considered.

1. Introduction

Measurements of the interplanetary magnetic field (IMF) in the solar wind upstream from the Earth are increasingly critical for improving our understanding of solar-terrestrial interactions and for operational space weather predictions. The most practical position for upstream monitoring is at the gravitationally stable first Lagrangian (L_1) position, ~230 R_E from Earth towards the Sun. Currently, NASA's Advanced Composition Explorer (ACE) satellite operates in a halo orbit around L_1, ~35 R_E from the Sun- Earth line. Interplanetary parameters measured near L_1 are acquired about an hour in advance of terrestrial effects. While ACE measurements are extremely useful, questions have been raised concerning the degree to which measurements taken off-axis near L_1 accurately represent the IMF that interacts with the Earth's magnetosphere. Previous investigations indicate that IMF measurements taken at wide off-axis separations do not always correlate very with those observed by satellites in the near-Earth solar wind.

The ISEE 3 satellite was launched in August 1978 into a wide halo orbit about L_1 to monitor approaching interplanetary structures capable of causing geospace disturbances [*Tsurutani and Baker*, 1979]. To predict whether such structures actually produce geomagnetic disturbances requires knowledge of how plasmas and fields passing L_1 correlate with near Earth values. The coherence of interplanetary parameters with distance from Earth has been studied with ISEE 3 near L_1at solar maximum and with the WIND satellite at various distances upstream near solar minimum. Most studies have focused separately on (1) IMF and (2) solar wind density/velocity structures. The main results may be summarized as follows:

In the first type of study, correlations between IMF structures observed upstream in the solar wind and near Earth range from good to poor [*Russell et al.*, 1980]. Good correlations are most frequently obtained if the IMF variability is high. When the IMF variability is low, good correlations are obtained if the distance perpendicular to the propagation direction $d_\perp < 20$ R_E [*Crooker et al.*, 1982]. *Russell et al.* [1980] suggested that the poorer correlations might reflect effects of propagating hydromagnetic structures in the solar

[1]N. C. Maynard, D. M. Ober, and D. R. Weimer, Mission Research Corporation, 589 West Hollis St., Suite 201, Nashua, NH 03062. (dweimer@mrcnh.com)
[2]W. J. Burke, Air Force Research Laboratory Space Vehicles Directorate, 29 Randolph Rd., Hanscom AF Base, MA 01731.
[3]M. R. Collier, Laboratory for Extraterrestrial Physics, NASA/GSFC, Greenbelt, MD 20771.
[4]D. J. McComas, Southwest Research Institute, P.O. Drawer 28510, San Antonio, TX 78228-0510.
[5]N. F. Ness, and C. W. Smith, Bartol Research Institute, University of Delaware, Newark, DE 19716-4793.

wind or that the surface normals to planes separating magnetic fields of different orientation make large angles to the ecliptic. By comparing the fraction of good IMF obtained with ISEE 3 and Wind near L_1 *Collier et al.* [1998] showed that coherence degenerates significantly near solar minimum. Through a probability analysis of observed advection times from L_1 to Earth, they demonstrated that phase-plane tilting rather than propagating magnetic structures were responsible for many apparent low correlations. A recent analysis of IMF measurements from the Wind, IMP 8, and Geotail spacecraft suggests that phase planes have radii of curvature of ~100 R_E [*Collier et al.*, 2001].

Ridley et al. [2000] used Wind and IMP-8 IMF measurements to estimate the uncertainty in the timing of propagation, using four different methods or assumptions to calculate phase front planes and the resulting time delays. They analyzed a number of individual events with sharp transitions where they was an unambiguous determination of the transition time between satellites, and found that the average uncertainty is 7.5-8.5 min for off-axis distances of 30 R_E, and at 100 R_E the uncertainties are 17.5-25 min. Using the total magnetic field vector to determine the front plane gave the lowest average error.

Lyons et al. [1997] had used IMF observations from both Wind and IMP-8 in conjunction with ground-based substorm observations in order to demonstrate evidence for substorm triggering. They found that "spatial structure in the plane perpendicular to the Earth-Sun line critically affects whether or not a trigger is observed for a particular IMF monitor; the probability of seeing a trigger for the substorms in our study is 89% for monitors that are < 30 R_E from the Earth-Sun line but only 50% for monitors 30 to 56.7 R_E from te Earth-Sun line."

In the second type of study, Solar wind fluxes, analyzed in 6 hr segments, showed good agreement between upstream and near-Earth measurements independent of the X_{GSE} and Y_{GSE} locations of the observing spacecraft [*Paularena et al.*, 1998]. *Richardson et al.* [1998] found that the best correlations between solar wind speeds and densities were obtained during periods of high variability in the density. A change in the correlation coefficients with X_{GSE} separation suggests that the solar wind evolved significantly across the 100 R_E diameter of ISEE 3's halo orbit about L_1. When sampling intervals were reduced to the 2 hr periods used in IMF studies, plasma correlations deteriorated to values less than those found for magnetic fields. *Richardson and Paularena* [1998] used three spacecraft to find the average east-west orientation of plasma structures in the solar wind. Using an analysis of 6 hr segments, they found that the average orientation of plasma fronts is roughly halfway between perpendicular to the solar wind and the Parker spiral direction. *Coplan et al.* [2001] compared solar wind fluxes observed by the SOHO (near L_1) and Wind spacecraft at large X_{GSE} and Y_{GSE} separations. The database extended from solar minimum (1996) to maximum (2000). Better correlations were observed near solar maximum. Again the concept of planar fronts proved useful in organizing the measurements, with the average surface normal in the quadrant of the Parker spiral.

Richardson and Paularena [2001] also used multiple spacecraft and compared correlations for both the plasma and IMF. They found a very strong dependence of correlation on spacecraft separation in the YZ plane. Scale lengths perpendicular to the flow, the distance over which the correlation decreases by 0.1, were 45 R_E for the IMF components, 70 R_E for plasma velocity and IMF magnitude, and over 100 R_E for density. Front orientations were similar for both plasma and IMF features.

Using data from the Sakigake satellite at 0.8-1.0 AU, *Nakagawa et al.* [1989] found periods lasting over 2 h that they called "planar magnetic structures," (PMS) characterized by variations in the magnetic field vector that were nearly parallel to a fixed plane. The plane includes the spiral direction but is inclined to the ecliptic plane from 30° to 85°. *Farrugia et al.* [1990] report observations of PMS oriented at a large angle, ~80°, to the Parker spiral, interpreted as produced by draping about a high velocity, compressed plasma cloud.

A complementary perspective on phase plane-propagation emerged from the analysis of electric fields detected during two rocket flights out of Svalbard in the midday magnetic local time (MLT) sector [*Maynard et al.*, 2000; 2001a]. At the times of the launches the Wind satellite was near GSM coordinates (200, 10, 25) R_E. IMF B_Z was northward during the first and southward during the second flight. In both cases B_X was the dominant component. Electric field variations in the ionosphere were compared with those in the interplanetary electric field (IEF) $E = V B_{YZ} \sin^2 \theta/2$. Here V is the solar wind speed, B_{YZ} is the projection of the IMF onto the GSM Y-Z plane, and θ is the clock angle of B_{YZ}. This representation of the IEF provides the maximum rate of component merging on the dayside magnetopause [*Sonnerup*, 1974]. Varying electric fields with similar waveforms were detected during the rocket flights and at locations Wind and IMP 8 satellites. In both instances the correlated signals were detected in the ionosphere well before expected advection times from L_1 to Earth. From the observed timing of IEF variations at Wind, IMP 8 and the approximate merging sites on the dayside magnetopause, *Maynard et al.* [2000; 2001b] estimated the tilts of phase planes that required significant rotations with respect to both the Y_{GSM} and Z_{GSM} axes.

Results of these previous studies, the majority of which have been based on long-period average observations, have implications for the accuracy of space-weather predictions using monitors in L_1 halo orbits. To investigate the question of accuracy in more detail, we had taken advantage of simultaneous measurements of the IMF available from four satellites, ACE, Wind, IMP-8, and Geotail. We had found that IMF measurements from all four satellites agreed much better than anticipated, when the advection lag was allowed to vary. Significant and highly variable changes in the delay times between the specific features observed at each satellite occur on time scales of minutes. This paper reports our initial findings concerning variable time delays.

2. A New Technique for the Accurate Determination of Time Delays

The importance of time delays is illustrated in Plate 1 which shows IMF measurements taken by ACE and Wind on January 21, 1999. Spacecraft locations are given in Table 1. The black lines in the top three panels of Plate 1 show the three GSE components of the IMF vector measured by ACE. In this and subsequent graphs, time lines on the horizontal axis are referenced to the times of measurements at ACE. In order to compare them with Wind measurements, it is necessary to compensate for time delays in solar wind propagation. The green line in the middle panel shows this advection/convection delay, calculated by dividing the separation distance along the GSE *X* axis by the *X* component of the solar wind velocity. The velocity was measured by the Solar Wind Electron, Proton, and Alpha Monitor (SWEPAM) on ACE [*McComas et al.*, 1998]. In this particular case the computed convection delay is relatively stable, at ~60 minutes. The green lines in top three panels show a superposition of the three components of the IMF vector measured by Wind, employing this convection delay. For example, at the 0800 UT position on the graph, IMF measurements from ACE were obtained at 0800 UT, and the IMF data from Wind were actually measured about an hour later at ~0900 UT. With this lag, the data agree poorly, and appear to have a negative correlation. However, when the Wind data are shifted in time by the proper lags they generally agree very well with the ACE data stream, as shown in the bottom three panels (although there are times where the match is not perfect). The ACE IMF measurements are again shown in black, and this time the Wind measurements are in blue. The actual lag time used to obtain this match is shown in blue in the middle panel. We refer to the lag that gives the best match between the two sets of vector measurements as the measured delay. The lag is not fixed. As seen in the graph it varies, ranging from ~60 min at 0130 UT to almost 150 min after 1300 UT. At this time it took the IMF 1.5 hr longer than expected to propagate from ACE to Wind. Note that the single variable lag usually brings the features of all three components of the IMF into agreement.

Such large variability in advection delays seriously impact our ability to understand magnetospheric interactions and predict space weather. We attribute the difference between the expected and actual advection delay times to planar IMF phase fronts whose surface normals are tilted at some angle with respect to the direction of the solar wind velocity vector. The positions of ACE and Wind at the mid-point of this interval, listed in Table 1, indicate that they had a larger separation in the Y_{GSE} direction (~84 R_E),which caused the tilted phase plane to reach Wind at the late time. As noted above, the concept of tilted phase planes is not new, [i.e., *Collier et al.*, 1998; *Maynard et al.*, 2000, 2001b; *Coplan et al.*, 2001], and *Maynard et al.* [2000, 2001b] found that the planes are also tilted in the XZ plane when a significant B_X is present. The fact that phase-front orientations and resulting lags varied continuously as functions of time was unexpected, with significant changes occurring within a few minutes. Variable time lags were not immediately obvious, and our method for calculating delays evolved during the research process. Our initial objective was to compare the IMF measurements of four satellites. It soon became apparent that measurements from all four satellites appeared to agree very well, with all significant features present, but only if the timings were adjusted. The first attempt to calculate the proper lags used fixed-width time intervals, of ~90 min, calculating the best lag for each interval. The resulting lag-versus-time graphs had stair-step forms with discontinuities at each step that seemed unnatural.

Rather than describe each step in our development, here we only outline the final algorithm for calculating the time lags. The process begins by dividing selected time intervals into sections, adjusting the lag time in each section from the previous value, and repeating the process using smaller and smaller divisions, while simultaneously decreasing the magnitude of the adjustments and improving the resolution. The time period shown in Plate 1 is used for purpose of illustration. Several steps in the sequence appear in Figure 1. To start the sequence, the advection delay time for the entire interval was used as the initial value of the measured delay function. This value was assigned to each of the 16 s resolution of ACE measurements of the IMF.

The initial interval was divided into 6 h segments, with the last segment extended to the end if the interval was not an even multiple of 6 h. An error value was calculated for each segment as follows. The time line at ACE is used as a fixed reference. The value of the delay function at each step is added to that time to obtain the delayed time at the target satellite. This time is in the future if the delay is positive. The ends of the segment may well be outside the range of the 6 h period under consideration. An interpolation of all IMF vector components that were measured at the target is used to obtain the IMF at the delayed times, one vector for each measurement in the original time series at ACE. The error is calculated by adding the square of the difference between each of the three vector components, accumulating the sum for every ACE data point in the segment.

For each segment a constant delay adjustment was found such that, when added to the previous delay function in that segment, the error between the IMF measured by ACE and the target satellite was minimized. This best delay offset was found by trying several possible values within an allowed range of offsets. For the initial segment period of 6 h, the tested offsets were in the range of -54 m to +54 m, or ±15% of the period. If the two best offsets were different by more than a desired resolution of 4.5 m (1.25% of the period), then several values between these best values were tried (this procedure is similar to a binary search). In essence this procedure finds the delay value that minimizes the least-square error between the three-vector series. After the optimal delay offset is found for a segment, the delay curve obtained with this offset replaces the original estimate for the data segment. The results after this first step are shown in Figure 1a. The boundaries of the 6 h segments are shown on the

illustration with the vertical lines. Discontinuities at the boundaries were smoothed with boxcar averaging.

The same procedure was repeated with segments that are 7/13 times the original length, or approximately 0.5385 h, with the results shown in Figure 1b. The range of offsets tested was again ±15% of the period, now ±29.1 m, and the resolution 2.42 m. The process was repeated a total of nine times. The results of steps 3 to 7 are shown in Figures 1c to 1g. After Figure 1d the segment boundaries are not shown for clarity, and the last two steps are not illustrated since the changes are not readily perceptible to the eye. The duration of the final segment is 2.54 m. After the sixth step the delay resolution is fixed at 8 s.

Some elements of this procedure were found by trial and error. The amount of detail or structure in the resulting delay function is sensitive to changes in the 15% factor. If it increased above 20%, the resulting delay fluctuations appeared unnatural. At one extreme, this routine can incorrectly match up IMF features with lag times of hours if it is not given reasonable constraints. On the other hand, if the allowed lag adjustments are decreased then the algorithm is not able to shift the delay time by a sufficient amount to match IMF structures that are easily visible to the eye. The original 6 h period was used so that the initial delay adjustment is approximately one hour, as required for extreme cases such as the one illustrated. Originally, segment periods were simply divided by two in each step, which sometimes resulted in unnatural features where boundary locations were aligned on sequential steps. The 7/13 factor insured that boundaries in one step usually would not match up with boundaries in other steps.

Several other details are worth noting. Conventional convolution techniques for determining lag times do not work, first because they must match three-component vectors, and second, lag times are not fixed throughout the interval. Additionally, the technique must work robustly when there are gaps in the measurements, as shown below. In our method, IMF values at the target satellite obtained by interpolation are not used in computing the total square error if the times fall within a gap in the original data. The average square error is actually used, dividing by the number of valid data points, to compensate for missing data. If at some point the number of invalid (within gaps) data points exceeds the number of valid points in a segment, then the delay function within that segment remains unchanged from its previous value. We do not claim that this method is necessarily the only and best algorithm for calculating the variable time delays, but it does appear to function correctly most of the time. It is not foolproof, as some adjustments in the parameters which might help the algorithm better match obvious features in some cases might cause it to fail in other cases, by matching up random noise fluctuations. The algorithm's performance is weakest when the IMF is relatively constant with small fluctuations.

3. Four-Satellite Comparisons

Our delay calculation technique has been applied to cases when solar wind/IMF measurements are available from the ACE, Wind, IMP-8, and Geotail at the same time. The sampling periods of the IMF data used here are 16.0, 3.0, 15.36, and 3.05 s from the four satellites, respectively. The 16 s data from ACE (Level 2) are available for nearly the entire period since operations began in early 1998. The algorithm was initially developed using coarse, but readily available Key Parameter, data from the other satellites, with sampling periods of 61 to 92 s. Only recently have high-resolution (3 s) IMF data from Wind become available to us, but only up to the period through the end of July 1999. For the cases shown here, higher resolution IMP-8 and Geotail data are likewise used. The 3 s data are smoothed with a 5-box sliding average before interpolation and comparison with the 16 s data due to their higher Nyquist frequency.

The time lag calculations are shown next for two of our four-satellite cases. Plates 2 - 4 show results from the first case spanning the period 1200 to 2400 UT on April 29, 1999. The format is identical to that of Plate 1, where the time axes on each of the three charts is referenced to IMF observations at the ACE satellite, shown with the black lines. As in Plate 1, the middle plot shows both the convection and measured delays, with green and blue lines, and the time-delayed target IMF data are shown in the upper three and lower three panels with superimposed green and blue lines. Breaks in the green and blue lines on these graphs, especially IMP-8 results, indicate gaps in the original data.

The results for the delay times at Wind in Plate 2 are quite different from those in Plate 1, as the measured and convection delays are similar. The reason is clear from the satellite positions indicated in Table 1, which show that Wind and ACE are not widely separated in the Y_{GSE} and Z_{GSE}. In contrast, the IMP-8 (Plate 3) and Geotail (Plate 4) lags show more significant differences between the measured and advection delays. IMF signals arrived at IMP-8 almost 20 m ahead of schedule. As indicated in Table 1, IMP-8 is the farthest from ACE in the combined Y-Z direction. If the lags are due to tilted phase fronts, then the greater the separations are perpendicular to the Sun-Earth line, the greater the discrepancy between the delays.

Plate 5 shows an example of IMF structure at high resolution. Measurements from all four satellites are superimposed for the 1 hr interval 2000 - 2100 UT, referenced to ACE, and using measured lags for the other three. The lines are colored to distinguish between the four, using black for ACE, red for Wind, green for IMP-8, and blue for Geotail. Note that there are 10 m between the major abscissa divisions and only 2 m between the minor tick marks. There are small-scale features of ~1 m or less that match at all four satellites even though the Y separation distances exceed 50 R_E. The period near 2030 UT is particularly noteworthy. There are matching structures that would not be fully resolved with sampling periods >16 s or if delay calculation did not have a similar accuracy. Such detail can be found in almost any time period chosen, and it is useful to know that IMF variations on a time scale of a minute are often coherent over Y_{GSE} separations of ~40 R_E.

The second case, spanning the period 1200 - 2400 UT on June 25, 1999, is shown in Plates 6 - 8. There are larger differences between the measured and convection delays with all target satellites due to their varied Y-Z separations, as indicated in Table 1. Variations in lags of ~ 20 m are common, and the sign of the actual delay with respect to the convection lag could change in minutes. Often time delays measured between ACE and the other satellites have very similar variations. As demonstrated in the next section there are differences between them that depend on the relative positions of the spacecraft and the orientations of the phase front plane.

Phase Front Orientation in Three Dimensions

Two dimensional phase front orientations were derived from observed time lags by *Collier et al.* [1998, 2000]. *Coplan et al.* [2001] also used three satellites to derive phase fronts in three dimensions, using lags of solar wind (plasma) flux averaged over 2 and 6 h periods. Here we calculate phase front orientations that vary on time scales of minutes, using four satellites. Normally three satellites are sufficient to derive a plane. While any three points will always fit a plane, this does not ensure that the plane has physical significance. Using four satellites provides a reality check for determining how well relative lags at locations of the four satellites agree with a planar structure. The short answer is that they generally fit very well.

The method used to determine orientations of phase fronts proceeds as follows. As all measured lag times are referenced to the time line at ACE, for each of the three target satellites the lag time from ACE is multiplied by the solar wind velocity measured at ACE at that instance. The resulting distances tells how far the plane must move along the velocity vector to get from ACE to each satellite. Each of the three satellites is then moved backwards along this vector to a "virtual" position, starting from where they were located at the moment when the IMF from ACE reaches them (the UT at ACE plus the measured lag times). All three components of the velocity vector are used for this translation. The resulting four points in space are then fit to a plane described by the equation

$$ax + by + cz + d = 0 \quad . \qquad (1)$$

The constants a, b, and c are direction cosines that satisfy the criteria

$$a^2 + b^2 + c^2 = 1 \qquad (2)$$

and d is the distance from the plane to the origin. The direction cosines also describe a unit vector that is normal to the plane. Equation (1) is solved for the four points for a least square error fit that minimizes the distance of all points from the solution plane, using the simplex method [*Press et al.*, 1986].

We have developed a computer visualization program which takes the results of time-delay calculations, carries out the above plane-fitting calculations, and show a simple three-dimensional view of how the phase plane is orientated at a given moment. Example results are contained in Plate 9, where the top four panels show different views of the same configuration at 1829 UT on April 29, 1999. Four spherical points, labeled A, W, I, and G, mark the relative locations of the spacecraft after the translations described above. The semi-transparent, gray surface represents the phase plane. It has been clipped to the edges of the viewing region extending from -50 to +90 R_E in the X direction and from -50 to +50 R_E in the Y and Z directions. If there were no differences between convection delays and the measured lag times from ACE, the phase plane would be perpendicular to the X axis.

An additional complexity has been introduced to the calculations described above to conform to our geocentric bias. The position of ACE was shifted forward to an X coordinate +40 R_E, upstream of the bow shock, and the virtual positions of the other satellites were adjusted accordingly. This way the Earth could be inserted into the picture (small blue sphere) to serve as a reference point. The different views in Plate 9, particularly where the plane is viewed from the edge, show that all four satellite do indeed fit a common plane very well. We find it difficult to make much sense of the time delay variations without such images.

Time lapse animations of this three-dimensional visualization have been produced for the full duration of the cases presented in Plates 2 - 4 and 6 - 8, and are provided as an electronic supplement to this paper. Watching how phase planes change orientation with time provides valuable insight on how well the four satellites fit a common plane, and how they all move in a coordinated manner consistent with the phase plane changes. Notable information is also gained by watching how the IMF vector changes in relationship to the measured phase plane orientation. These changing orientations must be considered for understanding magnetospheric interactions with the IMF. Plate 9 and the animations include fixed-length arrows at the location of the ACE satellite indicating the orientation of the IMF measured by ACE. We note that the IMF vector often, but not always, lies on or near the phase plane. At abrupt changes in the IMF direction the vector may lie within the phase plane both before and after the change while the phase plane remains nearly the same. This characteristic is illustrated in the bottom four panels of Plate 9 which shows different views of the configuration at 1839 UT, 10 m after the time considered in the top panels. The IMF underwent a significant change in direction, yet remained within the phase plane at nearly the same orientation as before. Similar IMF transitions have been examined at high resolution, and some are confirmed to be tangential discontinuities. Rotational discontinuities are also present in the IMF [*Turner and Siscoe*, 1971].

Based on the tendency seen in the animations, that the IMF vector lies in or near the phase front, it appears that a minimum-variance analysis [*Sonnerup and Cahill*, 1967; *Sonnerup and Scheible*, 1998] should give an indication of the phase front's orientation. A minimum-variance analysis was used by *Farrugia et al.* [1990] to deduce the orientation for one event, and *Ridley* [2000] showed that it can be used to reduce uncertainty in propagation times. We have had some success using the minimum variance technique, with ACE

data alone, to predict the phase front orientation angles that are measured with our 4-satellite technique. The minimum variance technique itself is prone to some uncertainty, and the accuracy can depend on an arbitrary choices of how many data points to use and the criteria for rejecting indeterminate eigenvectors. Using the results of 4-satellite cases, where the correct answers are known in advance, is essential to optimizing the minimum variance parameters and gaining confidence in the results. The details of these findings will be reported in a separate paper.

Graphs of phase-plane orientations as a function of time for both cases are shown in Figures 2 and 3. The three upper panels show the angles of the planes with respect to the X, Y, and Z axes, derived by taking the arcsine of the a, b, and c parameters. The values of a and the X tilt are always positive. A flat phase front with no time delay differences has the direction cosine a=1, as the plane's normal is aligned with the X axis, and the plane itself is tilted 90 degrees from X. Both Y and Z angles are zero in this case. Variations from these values correspond to tilted planes. Substantial directional changes are seen with time scales of the order of 10 min. Figure 3 is more interesting as it corresponds to a case with consistently larger time delay differences and hence large tilt angles. The tilt in the Z direction can be substantial, over 60 degrees at times, as shown in Plate 9. From what we have observed in this and other cases, substantial tilts in the Z direction are not uncommon, while the Y tilt tends to be more moderate. In comparing Figure 3 with Plates 6 – 8, we note that the Z tilt correlates inversely with the lag time to the Geotail satellite, which was the farthest away from ACE in the Z direction. At the same time there is a similarity between the Y tilt angle and the time delays to Wind and IMP-8.

Finally we turn our attention to the bottom panels in Figures 2 and 3, labeled RMS Error, R_E. This graph shows the square root of the mean squared distance from each satellite to the best-fit plane, the value minimized in the fitting procedure. It measures how well the positions of the four satellites, after lag translations, fit onto a common plane. Often this error is near zero, indicating a perfect fit. Even with degraded fits, the RMS error is rarely >4 R_E, the approximate distance that the solar wind travels in about one minute. For visual reference, the spheres in Plate 9 representing the satellites are 4 R_E in diameter. To obtain these kind of results it is necessary to have the time lags measured to a resolution much better than 1 minute, as we have done here. To verify that the good planar fits are not accidental, we have added random noise to the measured delay values, on the order to 2 to 4 minutes, with the result that good planar fits are destroyed and the angle and error graphs become very noisy. We can also see in Figure 2 that the error increases at ~1400 UT, the same time where gaps appear in the IMP-8 and/or Geotail IMF measurements. Much of the RMS error depicted on these graphs may also be due to wavy or spherical deformations in the phase fronts, as discussed by *Collier et al.* [2000].

The error calculations verify that lower errors are obtained if both the Y and Z components of the solar wind velocity, rather than X alone, are included in the satellite position translations. Fluctuations in the velocity vector cause the satellite positions in the animations to shift back and forth slightly in the Y and Z directions, and the positions of the satellites in Plate 9 therefore do not match the exact locations given in Table 1. With the translation of ACE to X = 40 R_E, its position is affected by the off-axis velocity fluctuations much more than the other three. The planar fit errors also indicate that better fits are obtained when the aberration of the solar wind, due to the Earth's orbital motion, is included in the Y component of the velocity vector. The aberration component is included in the results shown here, and it causes the virtual position of ACE to be shifted by about 15 R_E.

In *Russell et al.* [2000] it was asserted that there may be a time tagging offset error of about 70 s in the IMP 8 data, which has led to some concerns within the community. If such an offset existed, then the position of IMP 8 in our results would have been consistently shifted about 5 R_E in one direction. While we have not specifically searched for an error in the IMP 8 timings, such an offset is not seen in our three-dimensional animations, and the errors in the planar fits would have been larger.

4. Discussion and Summary

We have demonstrated that the propagation time of the IMF from an upstream monitor at L_1 may have significant and highly differences from the lag times that are calculated by using a simple propagation in the GSE X direction at the solar wind velocity. We have demonstrated a method to measure the actual propagation delay time from ACE to other satellites in the solar wind. A high temporal precision is obtained, which could not otherwise be achieved by conventional convolution techniques. This method has been used with four satellites to show that the results are consistent with nearly planar, tilted phase fronts, where the tilt angles vary on time scales of minutes.

The primary objective of this paper is to present these concepts and establish familiarity to them within the community. Additional, more detailed work can then follow, such as using a number of other four-satellite cases to better understand how often the phase planes are tilted and to what degree. Further study should concentrate on how well the IMF correlates from one satellite to another as off-axis separation increases, also as a function of scale size. ACE and Wind data alone are suitable for this study, but require applications of the technique presented here.

The impression gained from this work suggests that, with proper time-delay adjustments, the IMF correlations between different observation points are much better than expected. Thus, the probability is very high that the IMF measured at L_1 will impact the Earth's magnetopause. The important question concerns exactly when. Several implications follow from these findings. The first concerns the response time of the magnetosphere and ionosphere to IMF variations. *Ridley et al.* [1998] estimated that the delay time for ionospheric convection to begin reconfiguring after an IMF change impacts the magnetopause is ~8 minutes. It then takes about

12 more minutes to fully alter the convection pattern. *Maynard et al.* [2001a] showed that the 8 min reconfiguration delay was largely spent reversing the polarity of the cusp-mantle system of field-aligned currents. We note that the uncertainties in measurements reported by *Ridley et al.* [1998] were nearly as large as the average values. If the uncertainties reflect unknown planar tilts, using the techniques described here would likely reduce response-time variability considerably. Additionally, *Maynard et al.* [2001b] showed that tilted phase fronts impact the northern and southern merging regions of the magnetosphere at different times. As a result, different regions of the ionosphere in the same hemisphere may exhibit different lag times. With our more advanced phase front calculation tools it will be possible to make further progress in this subject.

Another area of impacted research concerns the timing of external substorm triggers. *Lyons et al.* [1997] and others argue that magnetospheric substorms are triggered by northward turnings of the IMF. This hypothesis has been often disputed on the basis of anecdotal cases where the timings between IMF variations and substorm onsets were not consistent. Results presented here shed a new light on the subject. Presumed trigger events may arrive at the magnetosphere much earlier or later than what was expected. Rigorous application of the technique described here can be used to help either definitively confirm or nullify the northward-turning hypothesis.

How to interpret or make sense of the variable tilts is a matter of conjecture. To begin with, the planar phase fronts are certainly approximations to large-scale, curved or undulating structures in the IMF. The orientation of the local surface normal changes as the curved surfaces move by. What we observe has similarities to the planar magnetic structures described by *Nakagawa et al.* [1989], but on a much smaller spatial and temporal scale. *Nakagawa et al.* [1989] interpreted their PMS events "as tongues of field lines or magnetic islands newly extended from the Sun or produced in interplanetary space." It is possible that the structures originating at the surface of the Sun to which *Nakagawa et al.* attributed the PMS produce magnetic field line structures near 1 AU at a multitude of scales.

Our findings have obvious implications for basic space-weather predictions. There had been some doubts about the reliability of IMF measurements at L_1 halo orbits for predicting effects at the Earth. Our findings strengthen confidence in our ability to predict geospace environments based on upstream measurements. There remains however a serious problem with this capability, in that there is an uncertainty in the timing of events. Times when an L_1 monitor is offset from the Earth-Sun line in the Z direction likely introduce worse timing errors than offsets in the Y direction; this conclusion is based on the three-dimensional phase plane pictures and the delay times from ACE to the other satellites when the targets were offset from ACE in the Z direction. Obviously, the multiple satellite time lag technique that is used in this paper cannot now be used for making predictions, as presently there is only one satellite transmitting solar wind data in real time. It would be ideal if the phase front orientation could be determined using real-time data from a single spacecraft in an L_1 orbit, or even closer to the Sun. As mentioned above, we have made some progress along these lines with the minimum-variance technique, to be the subject of a separate paper. We suggest here that the ideal solution would be to place three monitors at L_1, spaced 120° apart in their halo orbit so that tilts in the phase fronts can be determined. ACE is a research satellite, yet by its current use within NOAA and DoD forecast centers, it has demonstrated the need for operational weather satellites at L_1, and having three would also eliminate vulnerability to a single-point failure.

References

Crooker, N. U., G. L. Siscoe, C. T. Russell, and E. J. Smith, Factors controlling degree of correlation between ISEE 1 and ISEE 3 interplanetary magnetic field measurements, *J. Geophys. Res.*, *87*, 2224-2230, 1982.

Collier, M. R., J. A. Slavin, R. P. Lepping, A. Szabo, and K. Ogilvie, Timing accuracy for the simple planar propagation of magnetic field structures in the solar wind, *Geophys. Res. Lett.*, *25*, 2509-2512, 1998.

Collier, M. R., A. Szabo, J. A. Slavin, R. P. Lepping,, and S. Kokubun, IMF length scales and predictability: The two length scale medium, *Int. J. Geomagn. Aeron.*, *2*, 3, 2000.

Coplan, M. A., F. Ipavich, J. King, K. W. Ogilvie, D. A. Roberts, and A. J. Lazarus, Correlation of solar wind parameters between SOHO and Wind, *J. Geophys. Res.*, *106*, 18,615, 2001.

Farrugia, C. J., M. W. Dunlop, F. Geurts, A. Balogh, D. J. Southwood, D. A. Bryant, M. Neugebauer, and A., Etemadi, An interplanetary planar magnetic structure oriented at a large (-80 deg) angle to the Parker Spiral, *Geophys. Res. Lett.*, *17*, 1025, 1990.

Lyons, L. R., G. T. Blanchard, J. C. Samson, R. P. Lepping, T. Yamamoto, and T. Moretto, Coordinated observations demonstrating external substorm triggering, *J. Geophys. Res.*, *102*, 27,039, 1997.

Maynard, N. C., et al., Driving dayside convection with northward IMF: Observations by a sounding rocket launched from Svalbard, *J. Geophys. Res.*, *105*, 5245, 2000.

Maynard, N. C., G. L. Siscoe, B. U. Ö. Sonnerup, W. W. White, K. D. Siebert, D. R. Weimer, G. M. Erickson, J. A. Schoendorf, D. M. Ober, and G. R. Wilson, Response of ionospheric convection to changes in the interplanetary magnetic field: Lessons from a MHD simulation, *J. Geophys. Res.*, *106*, 21,429, 2001a.

Maynard, N. C., W. J. Burke, P.-E. Sandholt, J. Moen, D. M. Ober, M. Lester, and A. Egeland, Observations of simultaneous effects of merging in both hemispheres, *J. Geophys. Res.*, *106*, in press, 2001b.

McComas, D. J., S. J. Bame, P. Barber, W. C. Feldman, J. L. Phillips, and P. Riley, Solar wind electron, proton, and alpha monitor (SWEPAM) on the Advanced Composition Explorer, *Space Sci. Rev.*, *86*, 563, 1998.

Nakagawa, T., A. Nishida, and T. Saito, Planar magnetic structures in the solar wind, *J. Geophys. Res.*, *94*, 11,761, 1989.

Paularena, K. I., G. N. Zastenker, A. J. Lazarus, and P. A.Dalin, Solar wind plasma correlations between IMP-8, INTERBALL-1, and Wind, *J. Geophys. Res.*, *103*, 14,601, 1998.

Press, W. H., B. P. Flannery, S. A. Teukolsky, and W. T. Vetterling, *Numerical recipes: the art of scientific*

computing, 818 pp., Cambridge University Press, New York, 1986.

Richardson, J. D., and K. I. Paularena, The orientation of plasma structure in the solar wind, *Geophys. Res. Lett., 25*, 2097, 1998.

Richardson, J. D., and K. I. Paularena, Plasma and magnetic field correlations in the solar wind, *J. Geophys. Res., 106*, 239, 2001.

Richardson, J. D., F. Dasevisky, and K. I. Paularena, Solar wind plasma correlations between L1 and Earth, *J. Geophys. Res., 103*, 14,619, 1998.

Ridley, A. J., G. Lu, C. R. Clauer, and V. O. Papitashvili, A statistical study of the ionospheric convection response to changing interplanetary magnetic field conditions using the assimilative mapping of ionospheric electrodynamics technique, *J. Geophys. Res., 103*, 4023, 1998.

Ridley, A. J., Estimations of the uncertainty in timing the relationship between magnetospheric and solar wind processes, *J. Atm. Solar-Terrestrial Phys., 4*, 1, 2000.

Russell, C. T., G. L. Siscoe, and E. J. Smith, Comparison of ISEE 1 and 3 interplanetary magnetic field observation, *Geophys. Res. Lett., 7*, 381, 1980.

Russell, C. T., et al., The interplanetary shock of September 24, 1998: Arrical at Earth, *J. Geophys. Res., 105*, 25,143, 2000.

Siscoe, G. L., Structure and orientation of solar-wind interaction fronts: Pioneer 6, *J. Geophys. Res., 77*, 27, 1972.

Sonnerup, B. U. Ö, and L. J. Cahill, Magnetopause structure and attitude from Explorer 12 observations, *J. Geophys. Res., 72*, 171, 1967.

Sonnerup, B. U. Ö, Magnetopause reconnection rate, *J. Geophys. Res., 79*, 1546-1549, 1974.

Sonnerup, B. U. Ö, and M. Scheible, Minimum and maximum variance analysis, in *Analysis Methods for Multi-Spacecraft Data*, edited by G. Paschmann and P. W. Daly, Int. Space Sci. Inst., Bern, 1998.

Turner, J. M., and G. L. Siscoe, Orientations of 'rotational' and 'tangential' discontinuities in the solar wind, *J. Geophys. Res., 76*, 1816, 1971.

Electronic Supplements. There are two electronic supplements to this paper, consisting of computer animations. These animations show three-dimensional views of the IMF phase plane orientation as a function of time, for the duration of the entire intervals shown for the cases on April 29, 1999 and June 15, 1999. The format is the same as the pictures in Plate 9. Also shown are black lines drawn from each satellite to the nearest point on the best-fit phase plane, an indication of how well the four points lie on a common plane. For reference the animations also include on the right side a vertical graph of the IMF B_Y (green) and B_Z (red) measured at ACE, with a sliding blue bar that indicates the current time.

Table 1. Positions of the satellites for the three cases.

Date	Spacecraft	GSE Position (R_E)		
		X	Y	Z
Jan. 21,	ACE	236.0	32.9	13.6
	Wind	-13.1	-51.5	12.5
April 29,	ACE	224.5	-22.9	-16.4
	Wind	53.0	-19.3	-11.3
	IMP-8	15.5	29.4	-26.4
	Geotail	12.1	17.0	-2.9
June 6,	ACE	231.1	34.5	-13.8
	Wind	205.4	-21.1	-8.2
	IMP-8	34.6	-10.4	-18.0
	Geotail	22.3	8.4	-3.0

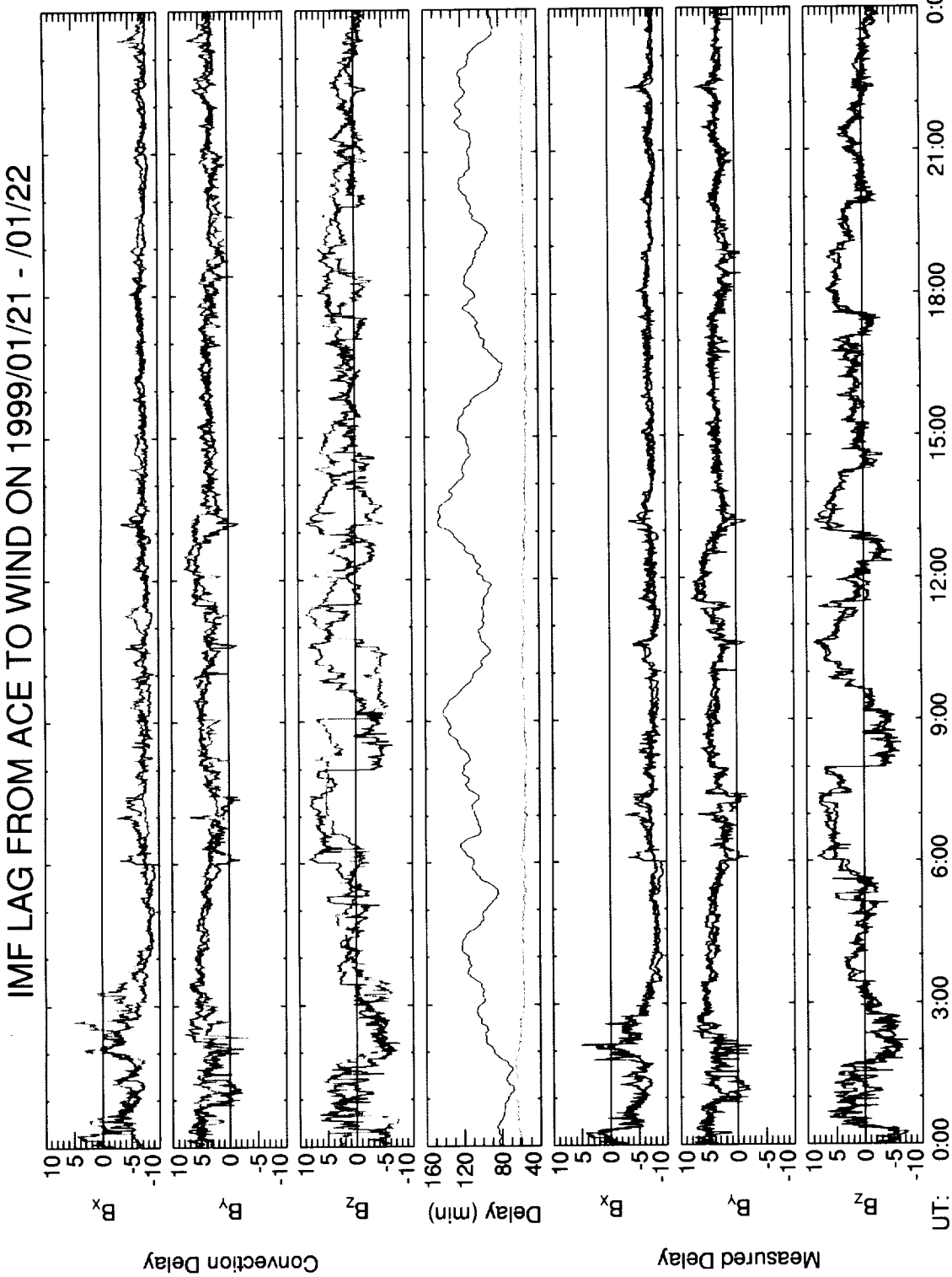

Plate 1. Interplanetary magnetic field (IMF) measured with the ACE and Wind satellites on January 21, 1999. The black lines in the three top and bottom panels show the ACE data. The green lines in the top three panels show the Wind data, with the measurements shifted in time according to the value of the advection delay, shown as the green line in the middle panel. The blue lines in the bottom three panels show the same data from Wind shifted in time by a variable amount that results in the best agreement with the ACE data. The lag time that produces this agreement is called the "measured delay," and is shown as the blue line in the middle panel.

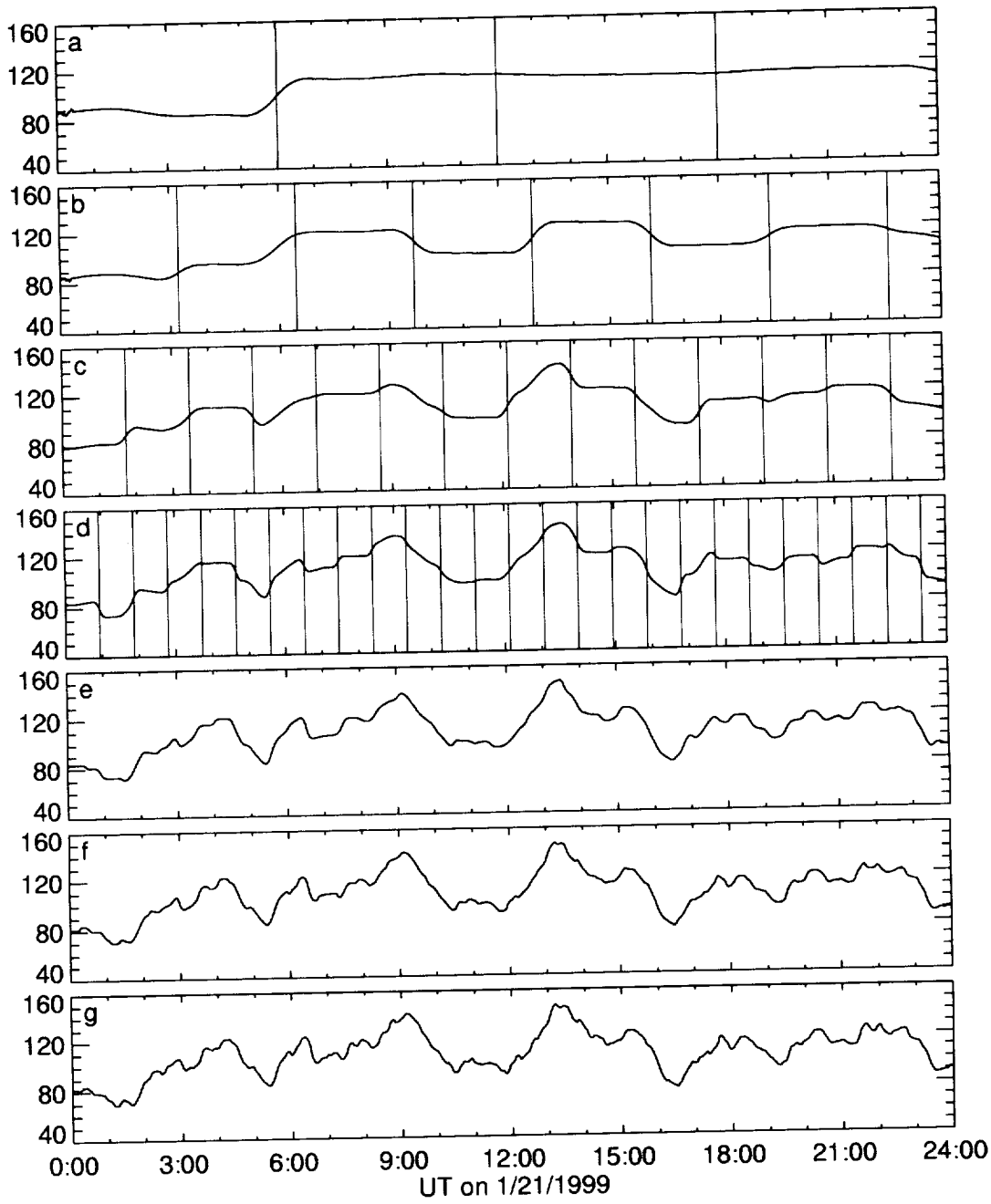

Figure 1. Example of the measured time delay as it evolves through the first seven steps of the calculation. The IMF data for this same interval are in Plate 1. The delay function is initialized with the advection value. In the first step (a) the entire interval is divided into 6 h segments, marked with the vertical lines, and the best delay offset from initial value is determined in each segment. The process is repeated, with the segment duration multiplied by 7/13 at each subsequent step while also increasing the resolution of the delay offset in each step. For clarity the segment boundaries are not shown after the first four steps.

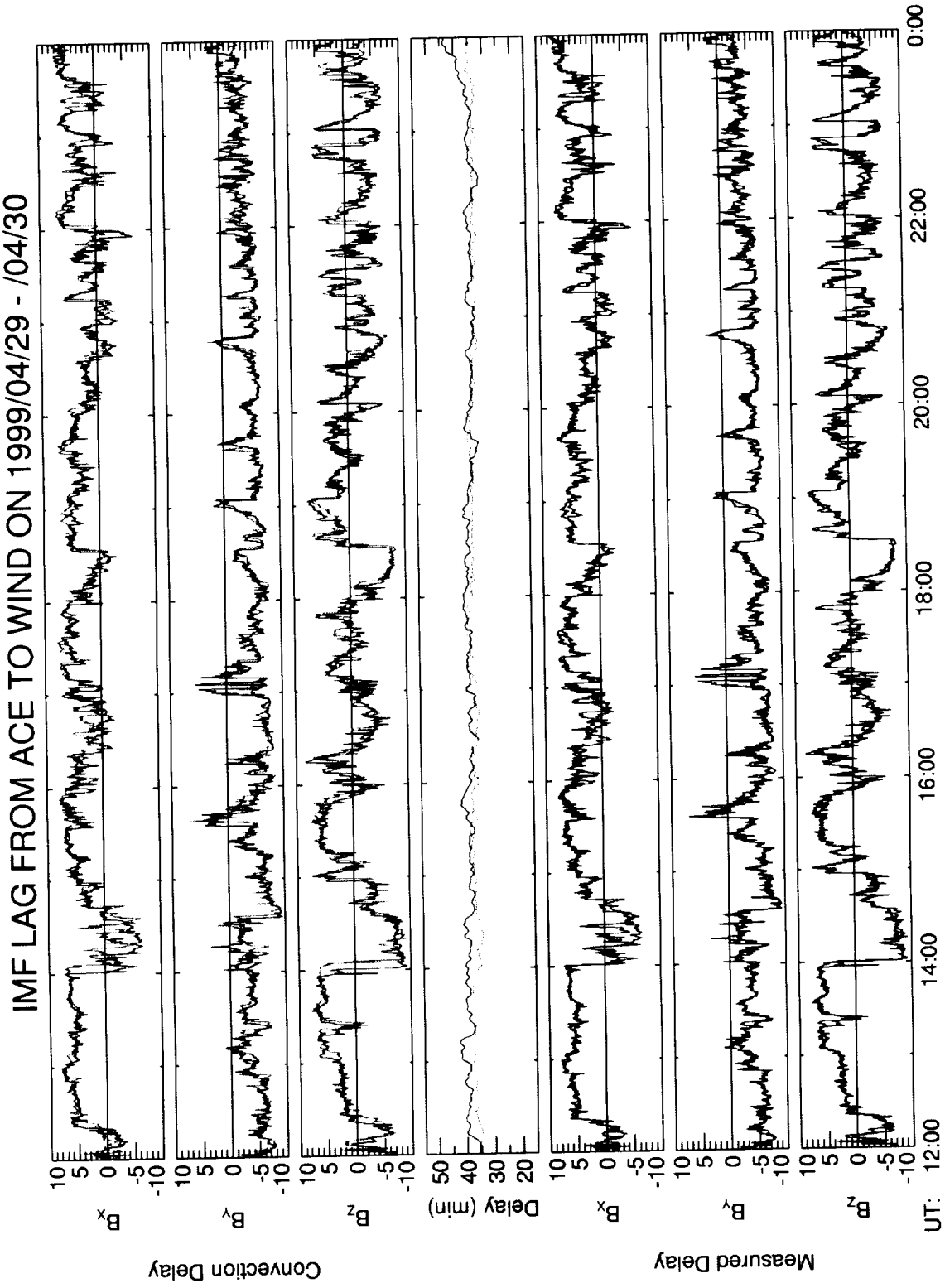

Plate 2. IMF measured with the ACE and Wind satellites on April 29, 1999. The format is the same as in Plate 1.

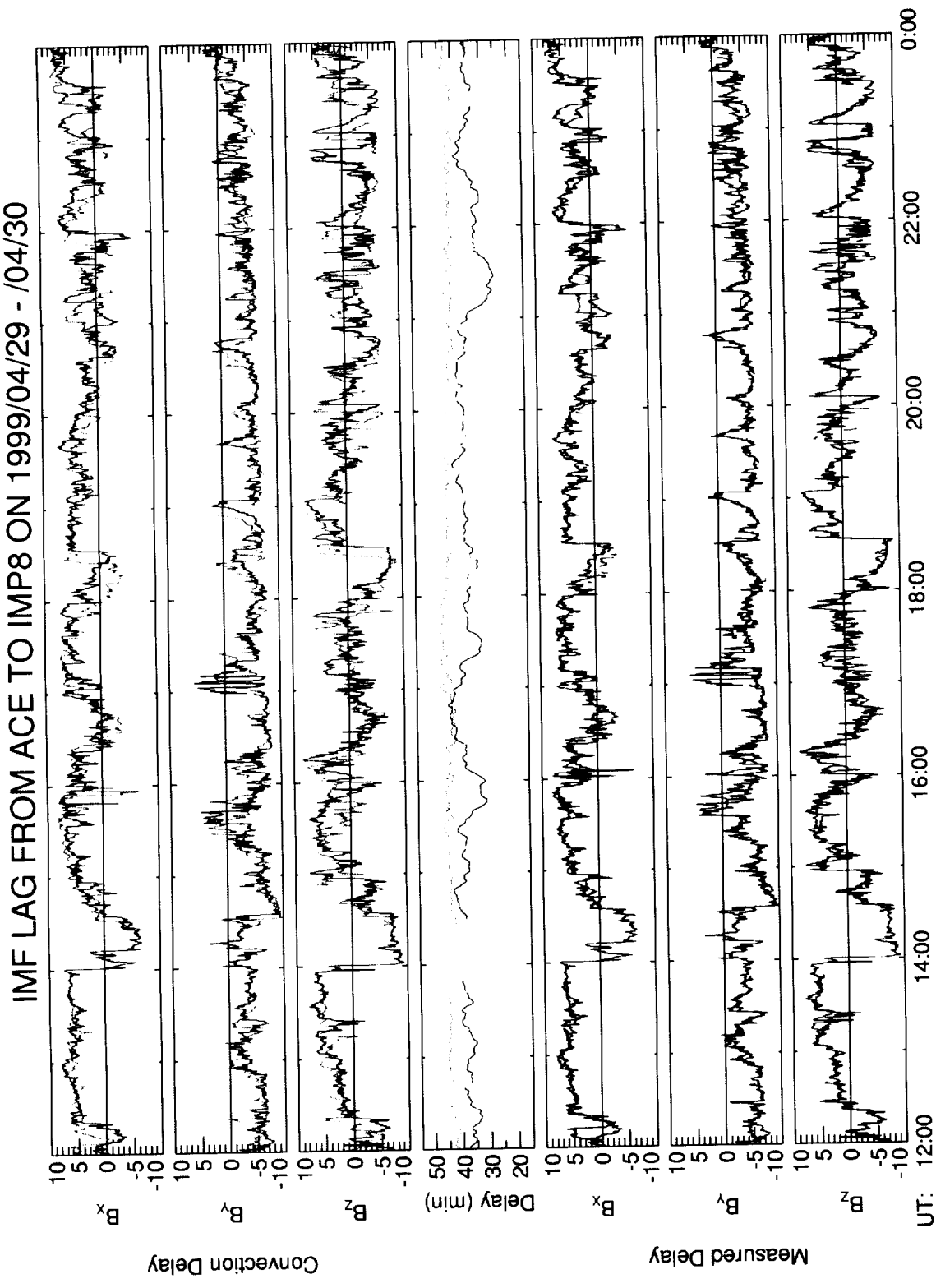

Plate 3. IMF measured with the ACE and IMP-8 satellites on April 29, 1999. The format is the same as in Plate 1, with the green and blue lines now showing the IMP-8 data. The gaps in the green and blue lines indicate where there were gaps in the IMF measured with IMP-8.

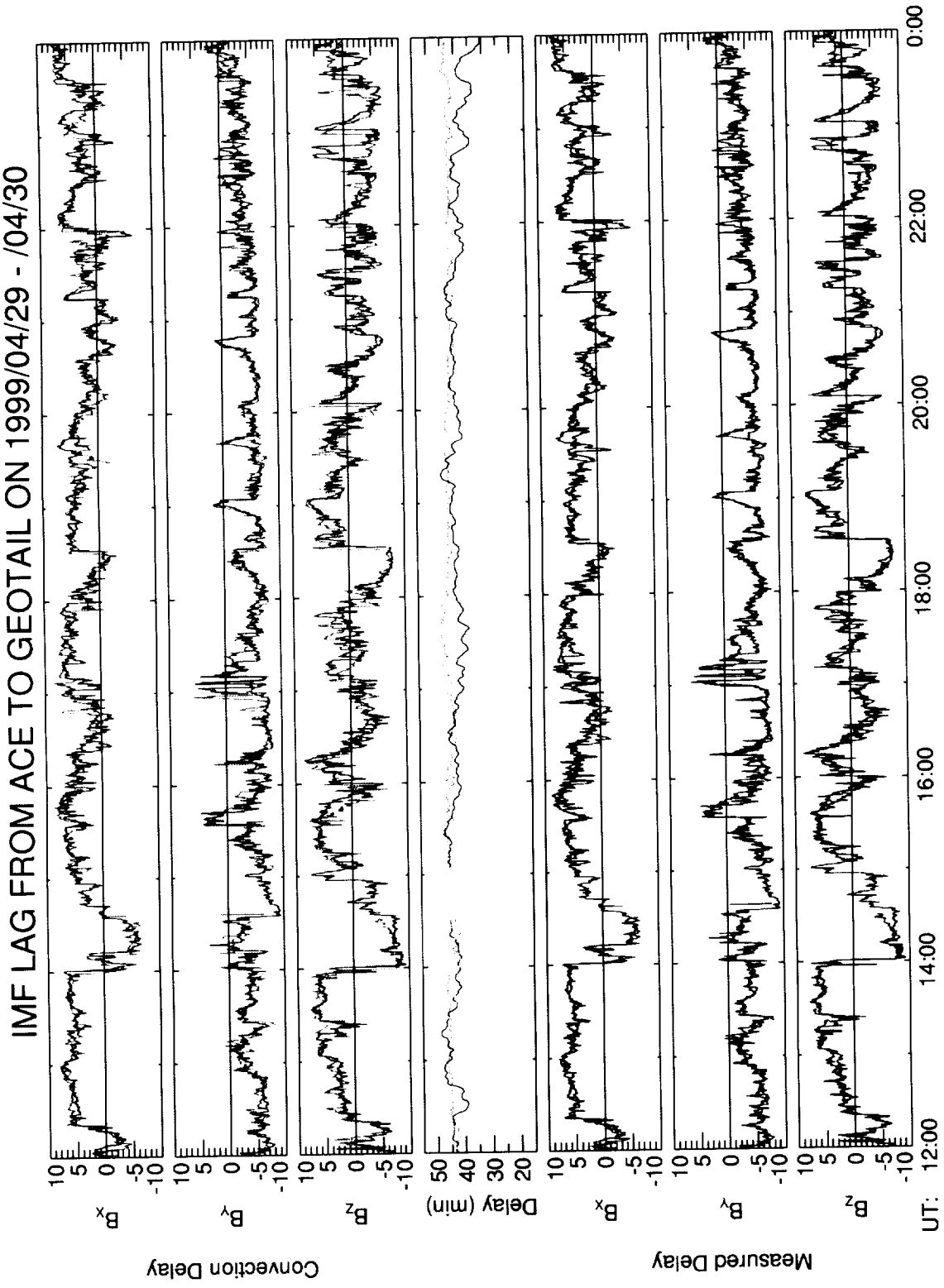

Plate 4. IMF measured with the ACE and Geotail satellites on

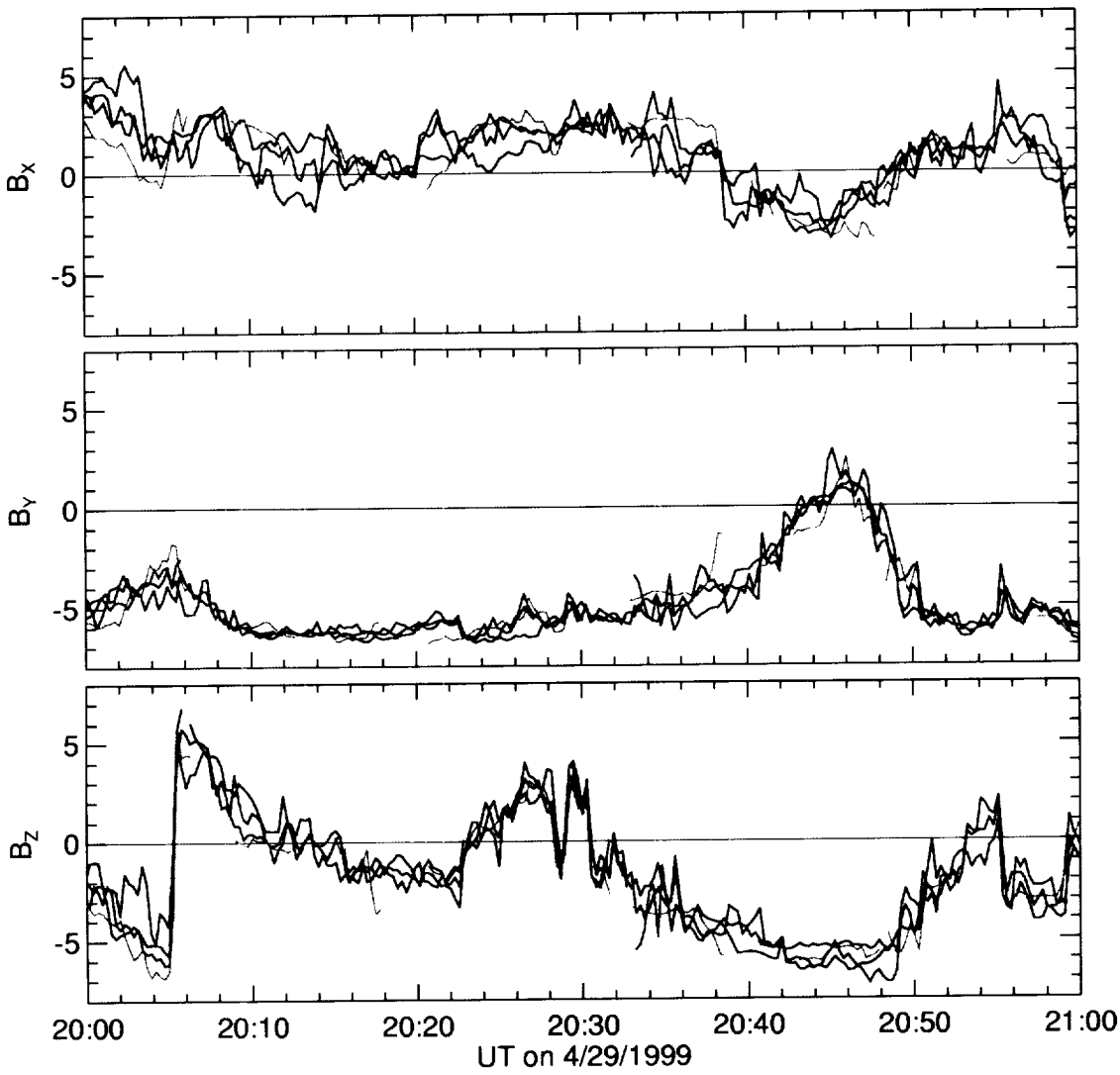

Plate 5. High-resolution graph of the IMF measured with all four satellites for a one hour interval on April 29, 1999. The data have been shifted according to the "measured" time delays, and are plotted on the same time scale as the ACE data, which are not shifted. The black, red, green, and blue lines show the data from ACE, Wind, IMP-8, and Geotail respectively.

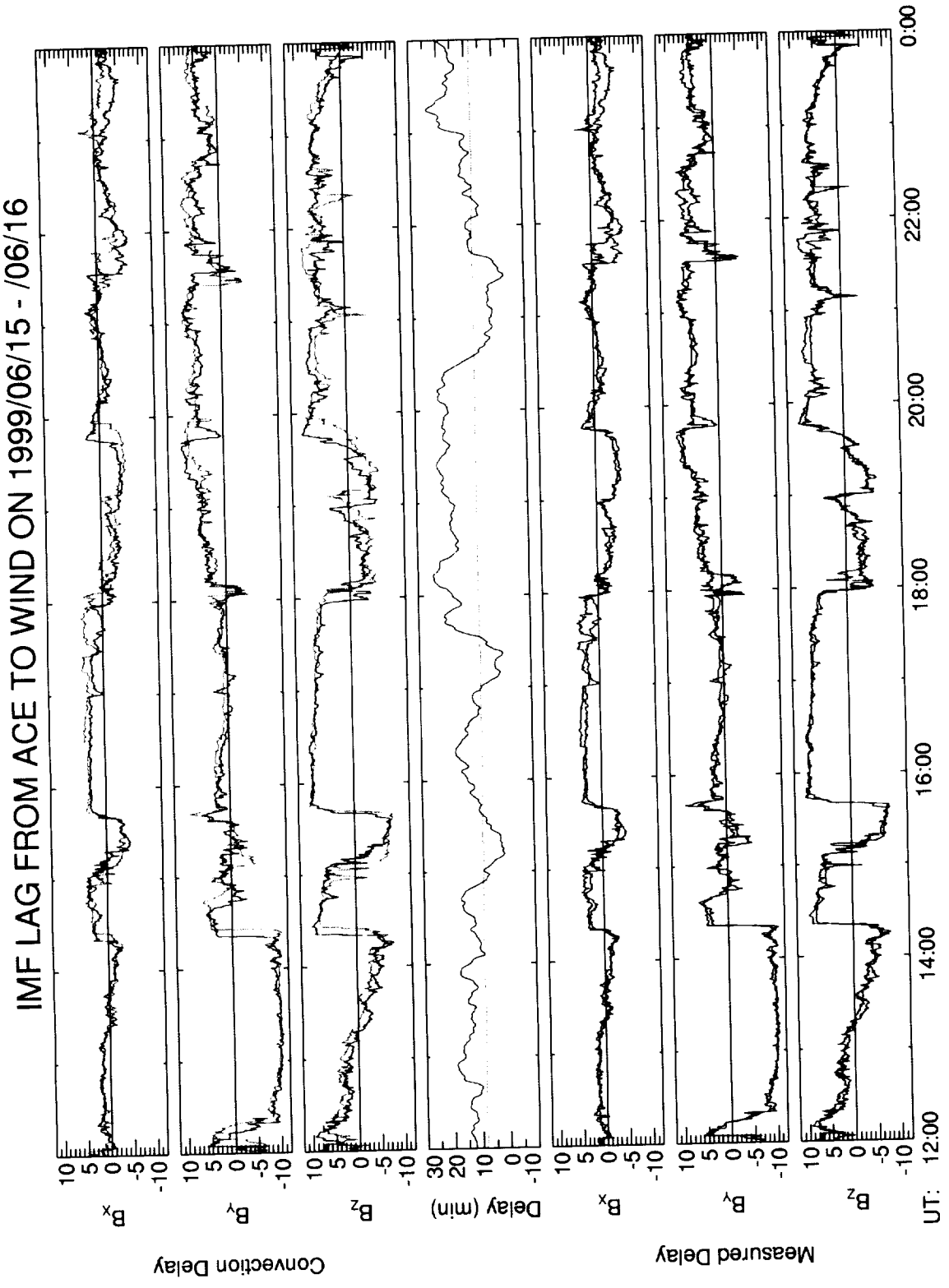

Plate 6. IMF measured with the ACE and Wind satellites on June 15, 1999.

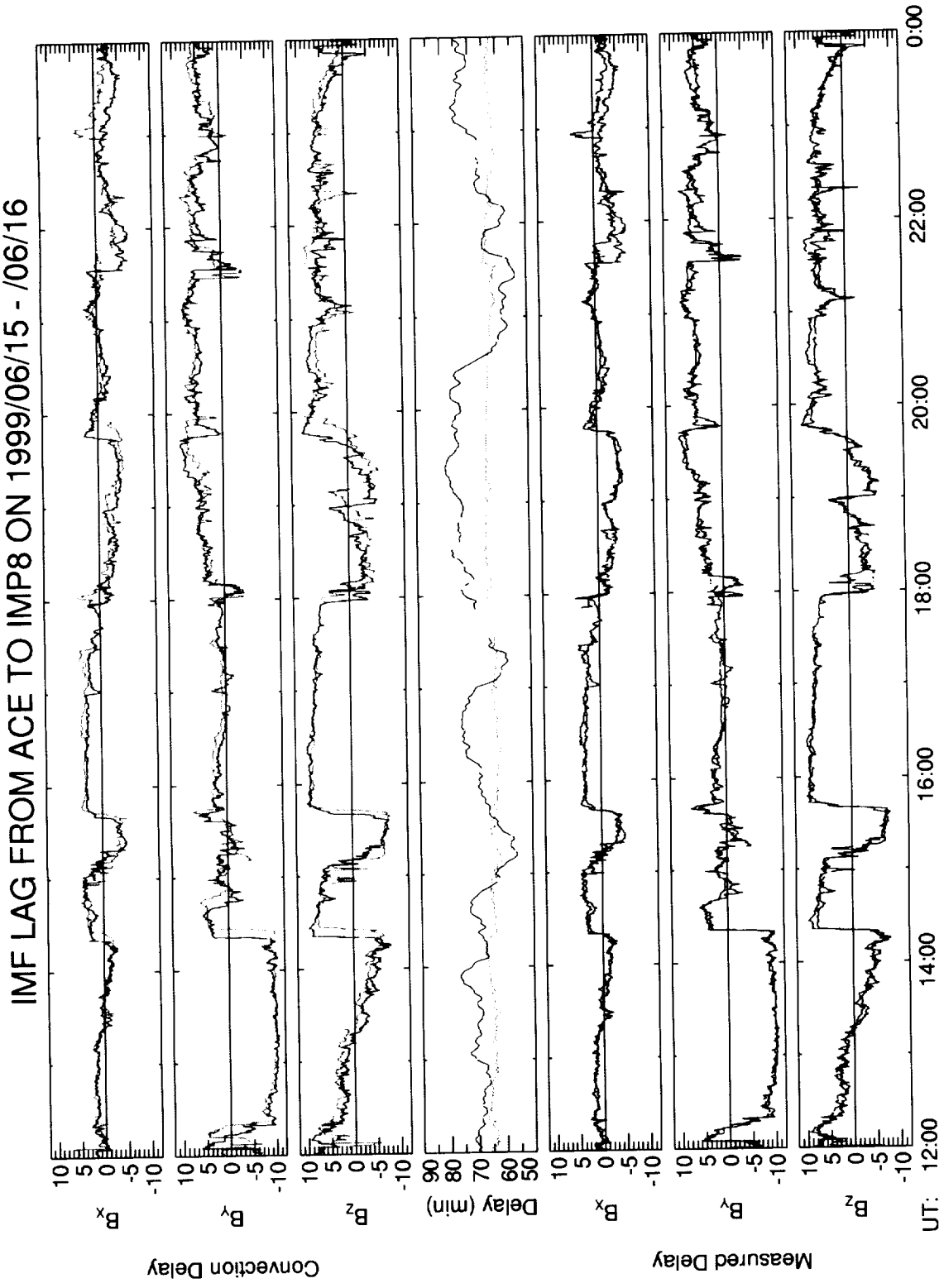

Plate 7. IMF measured with the ACE and IMP-8 satellites on June 15, 1999.

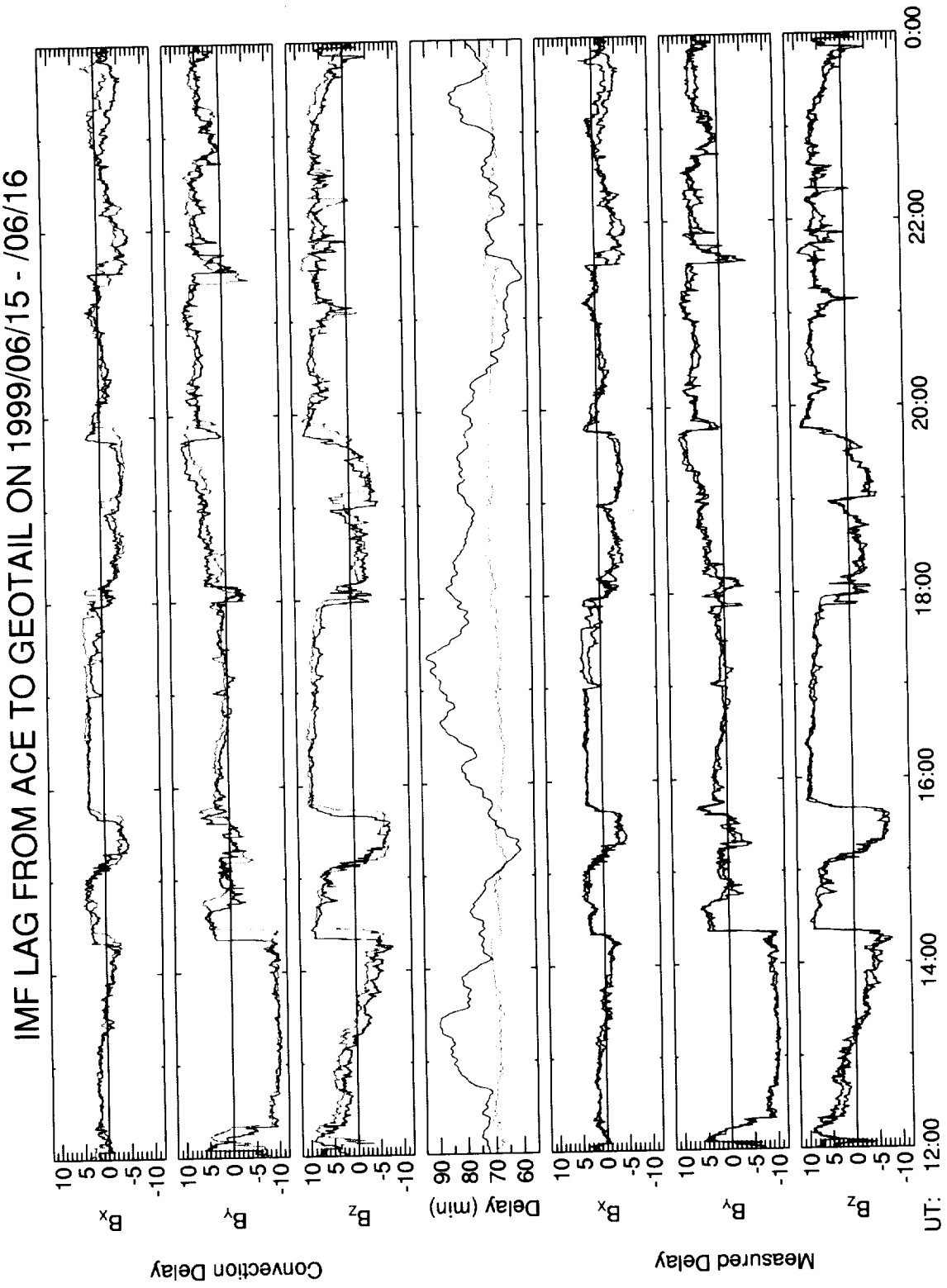

Plate 8. IMF measured with the ACE and Geotail satellites on June 15, 1999.

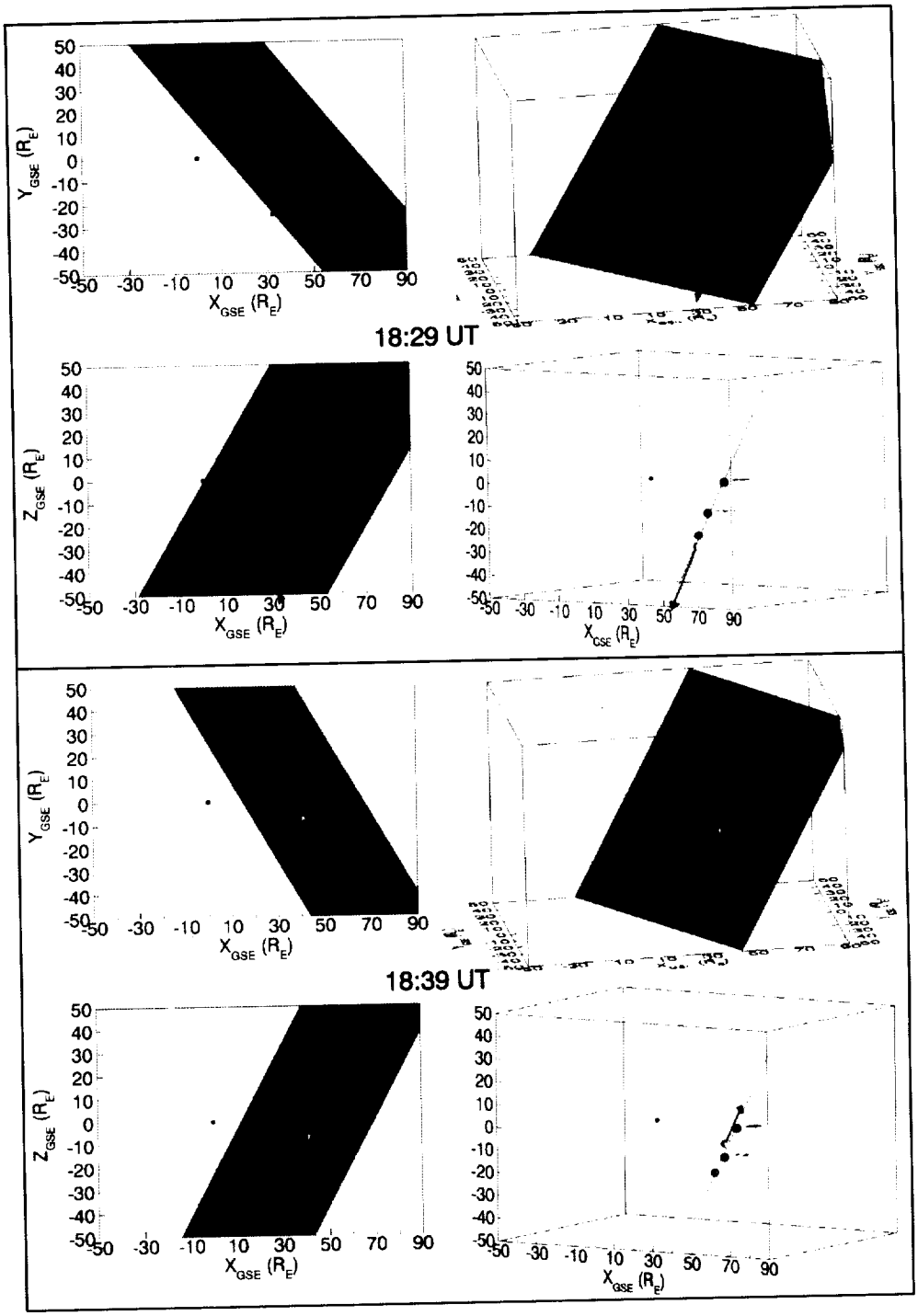

Plate 9. Three-dimensional views of the IMF phase plane orientation at two moments in time on April 29, 1999. The top four pictures show the phase plane from different viewpoints at 1829 UT, and the bottom four pictures show the same views 10 min later, at 1839 UT. The four colored spheres show the "virtual" locations of the four satellites, with the ACE satellite shifted forward up to X=40 R_E and the others shifted according to the measured delay times and solar wind velocity, compensated for the ACE shift. All shifts are along the velocity vector, measured at ACE. The spheres are labeled with the first initial of each satellite. These spheres are drawn with a diameter of 4 R_E. For reference, a blue sphere representing the Earth is shown at the origin. The arrow at the ACE location has a fixed length and points in the direction of the IMF vector measured at ACE. The phase plane orientation remains nearly the same while the vector reverses direction.

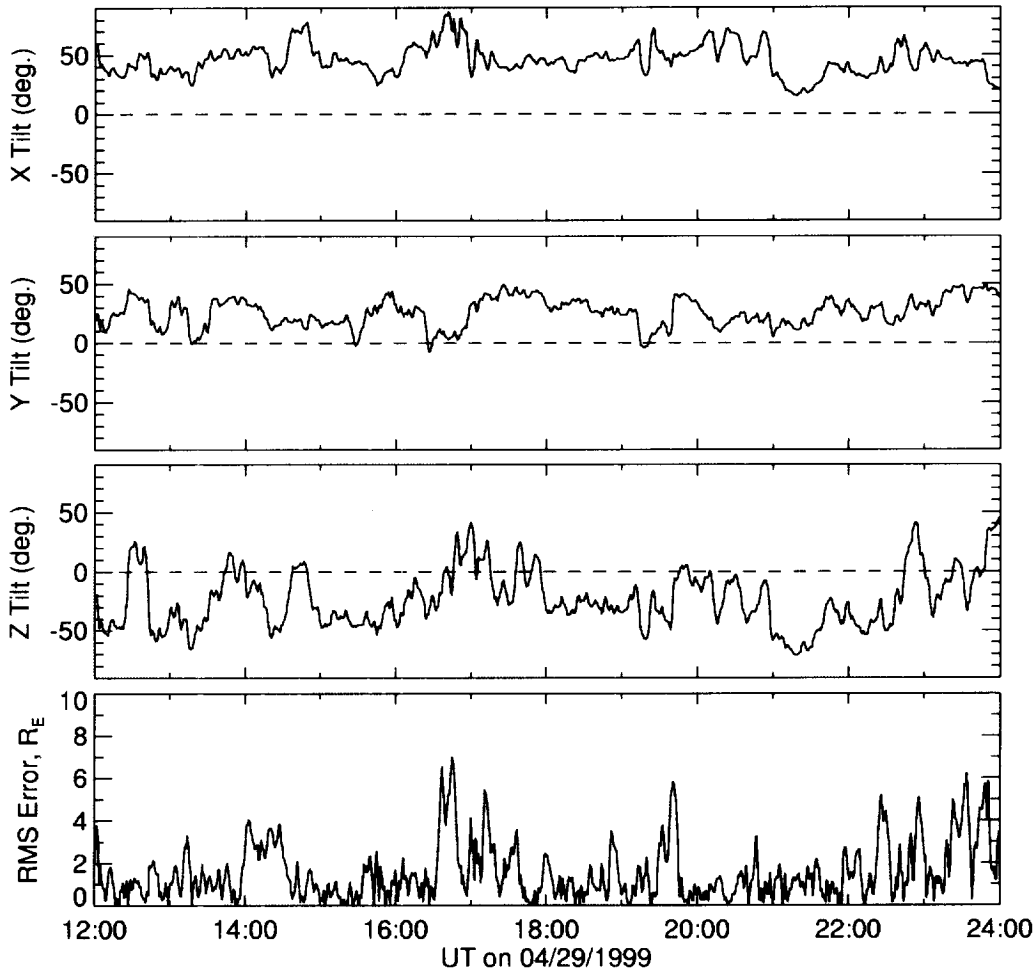

Figure 2. Graph of IMF phase plane orientation as a function of time for the case on April 29, 1999. The top three panels show the angle of the phase plane with respect to the GSE *X*, *Y*, and *Z* axes. The bottom panel shows the root mean square error for the fit of the four virtual satellite locations to a plane.

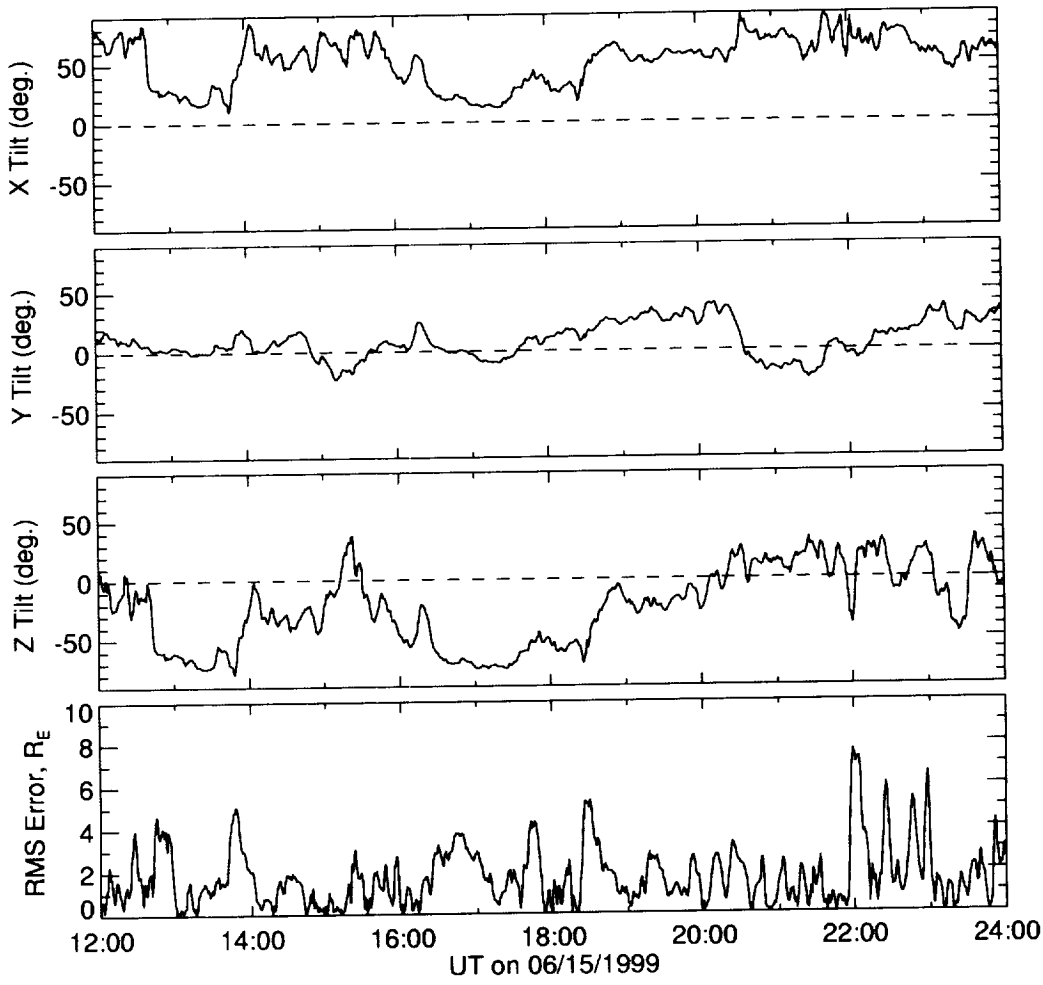

Figure 3. Graph of IMF phase plane orientation as a function of time for the case on June 15, 1999. The format is the same as in Figure 2.

Predicting IMF propagation delay times using the minimum variance technique

D. R. Weimer[1], D. M. Ober[1], N. C. Maynard[1], M. R. Collier[2], D. J. McComas[3], N. F. Ness[4], C. W. Smith[4], and J. Watermann[5]

(To be submitted to the *Journal of Geophysical Research*)

Abstract. Recently it has been shown that the propagation time of the interplanetary magnetic field (IMF) from the ACE satellite at L_1 to three other satellites may be significantly different from what would be expected by using a flat plane propagation at the solar wind velocity. The time differences can be accounted for by tilted phase planes in the IMF, where the angle of tilt varies on a time scale of minutes. A consequence of these tilted phase planes is that predictions of the effects of the IMF at the Earth, on the basis of the L_1 IMF measurements, will suffer from reduced accuracy in the timing of events. Since the multiple satellite technique cannot be used with real-time data from a lone satellite at L_1, then an alternative method is required to derive the phase front angles, which can then be used for more accurate space weather predictions. In this paper we show that the minimum variance analysis technique can be used to adequately determine the variable tilt of the plane of propagation. The number of points that is required to compute the variance matrix has been found to be much higher than expected, corresponding to a time period on the order of 30 to 40 minutes. The optimal parameters for the minimum variance analysis (MVA) were determined by a comparison with the results from the multiple-satellite time delay method. With use of the optimized parameters it is shown that the MVA method, using the ACE data alone, performs reasonably well for predicting the actual time lags in the propagation between ACE and other spacecraft, as well as to the Earth. Application of this technique can correct for timing errors, on the order of 30 minutes or more, in predictions of geomagnetic effects on the ground.

1. Introduction

Recently it has been shown that the planes of constant phase in the interplanetary magnetic field (IMF) are usually tilted at an angle with respect to the solar wind propagation direction, and that the tilt angle may often have significant variations on a time scale of a few minutes [*Weimer et al.*, 2002]. As a consequence of these changing tilt angles, the IMF that is measured by a spacecraft at one position in the solar wind will often arrive at another location with a propagation delay time that is earlier or later than that which would be calculated by assuming that all variations of the IMF are in a plane perpendicular to the Earth-sun line. The differences in the delay times were demonstrated by a comparison of the IMF measured by four different satellites, ACE, Wind, IMP-8, and Geotail, and a technique was developed where the differences in the timing between satellites could be used to calculate the actual orientation of the IMF phase front as a function of time. Another consequence of significance is that measurements of the IMF at the so-called first Lagrangian (L_1) position (~230 R_E from the Earth towards the Sun) are used extensively for research into the effects of the IMF on the near-Earth space environment, and for predicting these effects. These "space weather" predictions rely on the approximately one-hour propagation delay time, at the solar wind velocity, between the measurement at L1 (with essentially no delay in radio transmission) and the arrival of the same IMF at the Earth's magnetosphere. Due to the tilting of the phase planes, the timing of the IMF impact for both research and predictive applications will not be accurate unless the tilt is taken into consideration. This leads to a dilemma, as the technique of using multiple satellites can only be done at rare "conjunctions," and never in real time. Thus a technique is required for determining the orientation of the tilt angle using only the measurements from one satellite.

We have found that the "minimum variance analysis" technique [*Sonnerup and Scheible*, 1998] can be used to obtain a good estimate for the tilt angle of the phase plane. This technique had originally been devised for an analysis of data from satellite passes through the magnetopause boundary [*Sonnerup and Cahill*, 1967]. The technique had also been

[1]N. C. Maynard, D. M. Ober, and D. R. Weimer, Mission Research Corporation, 589 West Hollis St., Suite 201, Nashua, NH 03062. (dweimer@mrcnh.com)

[2]M. R. Collier, Laboratory for Extraterrestrial Physics, NASA/GSFC, Greenbelt, MD 20771.

[3]D. J. McComas, Southwest Research Institute, P.O. Drawer 28510, San Antonio, TX 78228-0510.

[4]N. F. Ness, and C. W. Smith, Bartol Research Institute, University of Delaware, Newark, DE 19716-4793.

[5]J. Watermann, Solar-Terrestrial Physics Division, Danish Meteorological Institute, Lyngbyvej 100, DK-2100 Copenhagen, Denmark.

used by *Farrugia et al.* [1990] for one event to deduce the orientation of the phase front in the IMF. *Ridley* [2000] showed that the minimum variance method could be used to reduce uncertainty in propagation times of distinct discontinuity events, and that it worked better than other, simpler methods such as flat plane propagation or using the orientation of the Parker spiral. Surprisingly, *Horbury et al.* [2001] had found that for tangential discontinuities the minimum variance technique had a very poor performance, and that better results were obtained with a cross-product of the magnetic field vectors on both sides of the discontinuity. *Horbury et al.* [2001] had used 60 s of IMF data on both sides of the discontinuities for their minimum variance calculations; it will be shown later that this number may have some influence on their results.

The purpose of this paper is to show the results of our investigation into using minimum variance in order to be able to improve upon the accuracy of the IMF propagation time delay. One very important criteria is that it is desired to have a method that could be as a matter of routine at all times, rather than usable only with distinct tangential discontinuity events.

2. The Minimum Variance Technique

To quote from *Sonnerup and Scheible* [1998], "the main purpose of minimum or maximum variance analysis (MVA) is to find, from single-spacecraft data, an estimator for the direction normal to a one-dimensional or approximately one-dimensional current layer, wave front, or other transition layer in a plasma." Without dwelling on the theory of the technique, which can be found in the references, it is useful to give a summation of the basic equations. With the elements of a symmetric, 3 by 3 "magnetic variance matrix" defined as

$$M^{B}_{\mu\nu} \equiv \left\langle B_\mu B_\nu \right\rangle - \left\langle B_\mu \right\rangle \left\langle B_\nu \right\rangle \quad , \qquad (13)$$

the fundamental MVA equation can be written in matrix form as

$$\sum_{\nu=1}^{3} M^{B}_{\mu\nu}\, n_\nu = \lambda\, n_\mu \quad . \qquad (13)$$

"The allowed values of λ are the eigenvalues λ_1, λ_2, λ_3 of $M^{B}_{\mu\nu}$ ... and the corresponding eigenvectors, $\boldsymbol{x}_1$, $\boldsymbol{x}_2$, and $\boldsymbol{x}_3$, are orthogonal. The three eigenvectors represent the directions of maximum, intermediate, and minimum variation of the field components along each vector" [*Sonnerup and Scheible*, 1998]. The eigenvector that corresponds to the smallest eigenvalue is in the direction of minimum variance and normal to the plane that contains the maximum variance, which is assumed to be the plane of the IMF phase front. Often the ratio of the intermediate to minimum eigenvalues is used as an indicator of the quality of the result. If they are approximately equal, so that this ratio is near unity, then the solution is said to be degenerate.

The MVA is prone to some uncertainty, and the accuracy can depend on arbitrary choices of both how many data points to use in computing the variance matrix and the criteria for rejecting degenerate cases. No definitive numbers are given in the references, although ratios in the range of 5 to 10 are often used as the requirement for a good, non-degenerate solution. However, by using the technique of the time delays measured between four different satellites [*Weimer et al.*, 2002], the correct results for the MVA are known, and comparisons of the two methods can be used to test how well the MVA technique works and how to optimize the parameters.

These comparison tests have been done for several of the four-satellite cases, where the minimum variance vectors are compared with the phase plane normal vectors determined by the multiple time delays. The IMF measured at ACE was used for the MVA calculations, since the major focus of this investigation has been to evaluate the reliability of the L_1 data for making predictions, and to develop techniques for improving these predictions. Initially it had been assumed that the MVA should be applied to data spanning just a minute or two of time, which may very well be the case for the magnetopause crossings for which this technique had been developed. But at first the MVA technique did not seem to work satisfactory. Then it was discovered that if the number of data points used to construct the magnetic variance matrix is greatly increased, then it does do quite well. For use with the typical IMF it was found that the number of data points that worked the best covered a time span on the order of 30 to 40 minutes. For example, using our highest resolution ACE IMF data, which are sampled at a cadence of 16 s, then the number that worked well was in the range of 115 to 130 sample points, corresponding to time spans of roughly 30 to 35 min. As the real-time data from ACE that are posted by the NOAA Space Environment Laboratory (SEL) are given at 1 min intervals, then the comparisons were also tried with similar data, using a 4-sample moving box average to resample the 16 s measurements at 64 s intervals. Now the number of data points required for the variance matrix was reduced to the range of 30 to 40, but the total time span comes out the same, if not a little longer. There are no precise numbers, as there were variations between the different cases on what worked the best.

Examples of two of these comparisons are shown in Figures 1 and 2, where the three stacked plots show the orientation of the phase plane normal vector (or minimum variance direction) as a function of time. What are plotted are the inverse sines, in degrees, of the normalized vectors' x, y, and z components in GSE coordinates. As the normal vectors that are calculated by either method have arbitrary signs, then each vector was multiplied by -1 if the x component were negative. Where the phase plane is not tilted at all, i.e. perpendicular to the Earth-Sun line and lying within the Y-Z plane, then the "X tilt" on the graph is 90 degrees and both the Y and Z tilt angles are zero. Alternatively, if the "Y tilt" increases in the positive direction, then it means that the normal vector is moving from the +X direction toward the +Y axis, and vice versa. The light grey lines on the two figures show the results using the multi-spacecraft time delay technique, with points computed at two minute intervals. The thicker black lines show the results from the MVA technique, in both cases using 30 points at the 64 s sample rate. The MVA computations would start with the first 30 points from

the time period, compute the variance matrix from these 30 points, and then test the matrix eigenvalues for degeneracy. If the intermediate/minimum eigenvalue ratio is greater than 2.5, then that minimum variance eigenvector is used for the phase plane normal direction; if the ratio failed this test then the previous "good" vector is used, up until a new one is found (hence the straight lines in some sections). Another criteria used to reject the "bad" orientations is that the normal should not be tilted more than 75 degrees from the X direction. The use of a "limiting angle" follows from Ridley [2000], who had used a 45 degree limit. The times of each MVA computation are at the center of each 30 point group. The computation steps forward in time by adding one new datum to the variance calculation and dropping the oldest one.

The ratio of 2.5 was also determined by the comparisons with the multiple-satellite results. If too high of a number is chosen for the minimum ratio, then a larger number of "good" points are eliminated as well as the indeterminate vectors, and the overall temporal resolution is reduced. If too low, then spurious spikes from the indeterminate results appear in the tilt angle plots. The optimal parameters for the MVA were derived by computing the dot product of the minimum variance vector with the normal vector that is obtained from the time delay method at the same time. This dot product is unity where there is perfect agreement. This dot product is computed for every MVA measurement within several events. The average of all dot products gives a figure of merit for each paired combination of the number points used and the minimum eigenvalue ratio. Figure 3 shows this figure of merit test score as a function of both the number of points used and the minimum eigenvalue ratio, evaluated on a two-dimensional grid. The MVA parameters are shown on the horizontal axes, and the score is shown as both a flat contour map and a vertical surface representation. The optimal combination is found where the figure of merit peaks, as indicated with the cross mark on the contour plot.

Although the vertical scale on this graph is exaggerated, it shows that the quality of the results starts to drop sharply as the number of data points that are used goes below 20 samples (at 64 s each). With 30 points there is a tendency for the score to drop as the minimum ratio is increased above 2.5. However, when few points are used the score increases as the ratio increases, so that a selection ratio in the range of 5 to 10 or more is not unreasonable, in agreement with the previously known guidelines.

Returning to Figures 1 and 2, it is seen that the results that are obtained by the two different methods, while not in perfect agreement, do match to a surprisingly high degree. The overlaid tilt angle graphs show that the same general trends in are present; the results from the MVA resemble a low-pass filtered version of the time delay results. There are also some sharp transitions that are present in the results from both methods at the same time. These results can be taken as a confirmation that the minimum variance method, when used with these parameters, does give a reasonably accurate measurement of the IMF phase plane tilt angle as a function of time. Conversely, the MVA results can be construed as a validation of the technique that is used to construct the time delays between satellites, and the subsequent interpretation of these variable delays as due to the tilting of phase front planes. In other words, comparable results are obtained from two entirely different techniques.

3. Further Validation Tests

Additional tests have been done to determine how well the MVA technique does at actually predicting propagation delay times, putting into practice the results from the prior section. One example is shown in Plate 1, which shows a comparison of the IMF that is measured by both ACE and Wind, for the same time period as was shown in Figure 2. The format of this graph is nearly the same as those that were presented by [*Weimer et al.*, 2002]. The upper three plots show the three components of the IMF measured by ACE in black on the original time line of these measurements at the ACE location. The green lines in these plots show a superposition of the same measurements at Wind, shifted backward in time to the ACE times according to the solar wind velocity and separation distance, and assuming a flat, non-tilted propagation. The green line in the middle plot shows the amount of this time shift, the solar wind "advection time delay," as a function of Universal Time. At the start of this time interval ACE was at coordinates (236.6, 38.8, -1.6) R_E GSE and Wind was at (208.5, -22.6, -0.7). As the separation between the two spacecraft in the X distance was small, the expected time delay is only a few minutes, yet there are places where the features in the green lines are obvious shifted in time ahead of the ACE results by up to 20 min. Due to the effects of the tilted phase planes, certain transitions in the IMF actually reached Wind before ACE, even though Wind was farther "downwind."

After computing the minimum variance directions as a function of time, using the ACE IMF measurements alone through the application of the procedure described above, the "predicted" propagation delay time from ACE to Wind is computed with the formula:

$$\Delta t = \hat{\mathbf{n}} \cdot (\overline{\mathbf{P}}_W - \overline{\mathbf{P}}_A) / \hat{\mathbf{n}} \cdot \overline{\mathbf{V}}_{SW} \qquad (13)$$

given the vector positions of Wind and ACE, the solar wind velocity vector, and the minimum variance eigenvector (the phase plane's normal direction), $\hat{\mathbf{n}}$. The blue line in the middle graph shows this propagation delay, and the blue lines in the bottom three panels show the Wind IMF measurements shifted in time accordingly, overlaid on the same reference ACE measurements in black. The MVA technique performed reasonably well at predicting the actual lag times, as transition features in the IMF that did not line up before now come together quite nicely. For purpose of comparison, the red line in the middle graph shows the time delay that achieved the greatest match between the IMF measurements, using the technique described in detail by *Weimer et al.* [2002]. Because these spacecraft are separated by 61.4 R_E in the Y direction, and almost none in the Z direction, these time delays follow the Y tilt angle shown in Figure 2. Similar results were obtained with other cases, including the example case shown in the prior publication from January 21, 1999

where the time lags were well over an hour greater than expected due to a very wide separation between ACE and Wind.

Next it seems prudent to ask whether or not the tilted phase planes can have any significant influence on space weather predictions, since ACE's separation from the Earth-Sun line, about 40 R_E, is not as great as from Wind in the extreme example cases. The answer is found by performing the MVA and delay calculations with the ACE data for a number of different days. The result is that while the differences in the delay times are not as great, and often the difference between the normal and tilted propagation times is negligible, it is still not uncommon for there to be differences on the order of 30 to 40 minutes. An example is shown in Figure 4, where the bottom three panels show the predicted tilt angles in the same format as in the previous figures. An additional panel on top shows the computed time delays from ACE to Earth using both the MVA technique with the heavy black line and the flat plane calculation as the lighter gray line. For this calculation the position of Wind in (3) was replaced by a "target" point on the Earth's magnetopause near the Northern cusp, at (8, 0, 4) R_E.

This case in Figure 4 from June 6, 2001 is one of several found in an examination of very recent ACE data during Northern summer months where there was both a significant difference between the two delay calculations and a distinct transition feature in the IMF which would be detectable by the response of high-latitude magnetometers on the ground. The objective was to test the MVA technique with an actual "space weather" prediction without using any other IMF data from a second spacecraft. In Figure 5 are shown the *Y* and *Z* components of the IMF, from 10 to 14 UT, as a function of the predicted times of impact on the magnetopause. The light gray lines show the result using the non-tilted delay calculation and the heavy black lines use the MVA results. There is an approximately 30 min time difference in the arrival of the transition where the Y component goes briefly positive, while the Z component swings from positive to negative, back to positive, and again to negative. As the MVA time delays are not constant, some features of the IMF are not just shifted in time but have their temporal profile altered as well.

In Figure 6 are shown both the northern and vertical components of the magnetic perturbations measured from four northern stations in the "Greenland Chain" that is maintained by the Danish Meteorological Institute. The corrected geomagnetic latitudes of these stations are in the range of 76.8 to 83.5 degrees. The actual magnetometer data are shown as the light gray lines, the same in both rows. As it is not obvious what the effects should be from the IMF shown in Figure 5, in order to facilitate a comparison these data have been passed through a model which can predict magnetic perturbations solely on the basis of the IMF, solar wind velocity, and the dipole tilt angle (which includes the seasonal effects). The heavy black lines in Figure 6 show the model perturbations, with the bottom row using the IMF from the flat plane propagation and the top row using the tilted phase fronts from the MVA technique. It is evident that the timing of the comparison is very good in the top row, with the MVA technique, while in the bottom row the predicted effects of the IMF occur about a half-hour before they are actually seen.

The prediction of these geomagnetic effects were derived from an interim version of the empirical field-aligned current model described by *Weimer* [2001]. The exact details of how the geomagnetic prediction is accomplished with this particular model is beyond the scope of this paper and will be described in more detail in a future publication. Suffice it to say, the technique is akin to the reverse of the well-known magnetometer inversion process to derive the field-aligned currents [*Richmond*, 1992]. The exact values of this model are not as important as the timing of the characteristic signature that is associated with this particular flip in the IMF.

Thus the tilting of the phase planes is demonstrated to have a measurable influence on the propagation of the IMF from their measurement at the L_1 location to the Earth, and it would be advantageous to always use an MVA calculation when these time delays are required, for both research purposes and actual forecast predictions. Although the technique is not 100% accurate and foolproof, the overall results should be more accurate than not doing any correction at all for the tilted propagation.

There is one other minor point worth mentioning. All three components of the solar wind velocity are used in (3) for calculating the proper delay time. Even though the X component is by far the most important, the other two components were found in to previous study to have subtle contributions as well. It is also worth repeating that the spacecraft at the L_1 orbit share with the Earth an orbital motion around the Sun, and this creates an aberrated component to the solar wind velocity in the +Y direction that is seen in the spacecraft velocity measurements. This aberration is routinely removed in the processing of these velocity measurements, so that the data are transformed to the reference frame of the Sun. When these data are given in GSE coordinates, the angular rotation to this coordinate system is done without the translation of the velocities to the Earth-centered reference frame. For the purpose of calculating the delay times in three dimensions the aberration needs to be put back in, which amounts to adding 29.8 km/s to the Y component. Over the course of an hour this correction changes the Y position by about 17 R_E, or almost half the radius of the ACE libration orbit around L_1. In the case of the real time data from ACE, currently only the X component of the velocity is supplied, so that the Y component should be given an assumed value of 29.8 km/s rather than zero.

4. Discussion and Summary

Previously it had been found that the propagation time of the IMF from an upstream monitor at L_1 to other satellites may be significantly different from what would be expected by using a simple, flat plane propagation in the GSE X direction at the solar wind velocity. The differences can be accounted for by tilted phase planes in the IMF, where the angle of tilt varies on a time scale of minutes. A consequence of these tilted phase planes is that predictions of the effects of the IMF

at the Earth on the basis of the L_1 measurements may suffer from reduced accuracy in the timing of events. A technique for measuring the actual delay times between multiple satellites was used to determine the angle of tilt and how it varies with time. As this technique can not be used with real-time data from a single satellite at L_1, then an alternative method is required to derive the phase front angles for more accurate space weather predictions.

In this paper we have demonstrated that the minimum variance analysis technique can be used to adequately determine the variable tilt of the plane of propagation. The number of points that is required to compute the variance matrix had been found to be much higher than expected, corresponding to a time period on the order of 30 to 40 minutes. This number most likely is related to a characteristic scale size of the solar wind IMF, and it is not expected to be valid for other applications of the minimum variance technique.

The optimal parameters for the MVA were determined by a comparison with the results from the time delay method, in several cases having multiple-spacecraft IMF measurements. With use of the optimized parameters it has been shown that the MVA method, using the ACE data alone, performs reasonably well for predicting the actual time lags in the propagation between ACE and other spacecraft as well as to the Earth. It has been shown that this technique can correct for timing errors, on the order of 30 minutes, in predictions of geomagnetic effects on the ground. We note that, in addition to use with empirical models, this technique should also be usable for improving the performance of MHD simulations, although it is recognized that there is considerable complexity involved in implementing a variable-tilt IMF phase front in such models. Perhaps even the empirical models could be made more sophisticated in order to mimic the recent findings by *Maynard et al.* [2001] that the tilted phase planes will interact with the northern and southern hemisphere merging regions at different times, and the effects in one hemisphere are later seen in the other. It would first be required to know the tilt angles, which the MVA provides, but currently it is not known how to incorporate the "double source" effects in an empirical model.

For an analysis of events which are clearly tangential discontinuities, the cross-product method described by *Horbury et al.* [2001] may very well be more suitable. But for more general use, where the tilt angles are required at all times, the MVA technique can be used to advantage for more accurate timing of IMF propagation and the subsequent predictions.

References

Farrugia, C. J., M. W. Dunlop, F. Geurts, A. Balogh, D. J. Southwood, D. A. Bryant, M. Neugebauer, and A., Etemadi, An interplanetary planar magnetic structure oriented at a large (-80 deg) angle to the Parker Spiral, *Geophys. Res. Lett., 17*, 1025, 1990.

Horbury, T. S., D. Burgess, M. Fränz, and C. J. Owen, Prediction of Earth arrival times of interplanetary southward magnetic field turnings, *J. Geophys. Res., 106*, 30,001, 2001.

Maynard, N. C., W. J. Burke, P.-E. Sandholt, J. Moen, D. M. Ober, M. Lester, and A. Egeland, Observations of simultaneous effects of merging in both hemispheres, *J. Geophys. Res., 106*, 24,551, 2001.

Richmond, A. D., Assimilative mapping of ionospheric electrodynamics, *Adv. Space Res., 6*, 59, 1992.

Ridley, A. J., Estimations of the uncertainty in timing the relationship between magnetospheric and solar wind processes, *J. Atm. Solar-Terrestrial Phys., 4*, 1, 2000.

Sonnerup, B. U. Ö, and L. J. Cahill, Magnetopause structure and attitude from Explorer 12 observations, *J. Geophys. Res., 72*, 171, 1967.

Sonnerup, B. U. Ö, and M. Scheible, Minimum and maximum variance analysis, in *Analysis Methods for Multi-Spacecraft Data*, edited by G. Paschmann and P. W. Daly, Int. Space Sci. Inst., Bern, 1998.

Weimer, D. R.,Maps of field-aligned currents as a function of the interplanetary magnetic field derived from Dynamics Explorer 2 data, *J. Geophys. Res.,106*, 12,889, 2001.

Weimer, D. R., et al., Variable time delays in the propagation of the interplanetary magnetic field, *J. Geophys. Res.,107*, in press, 2002.

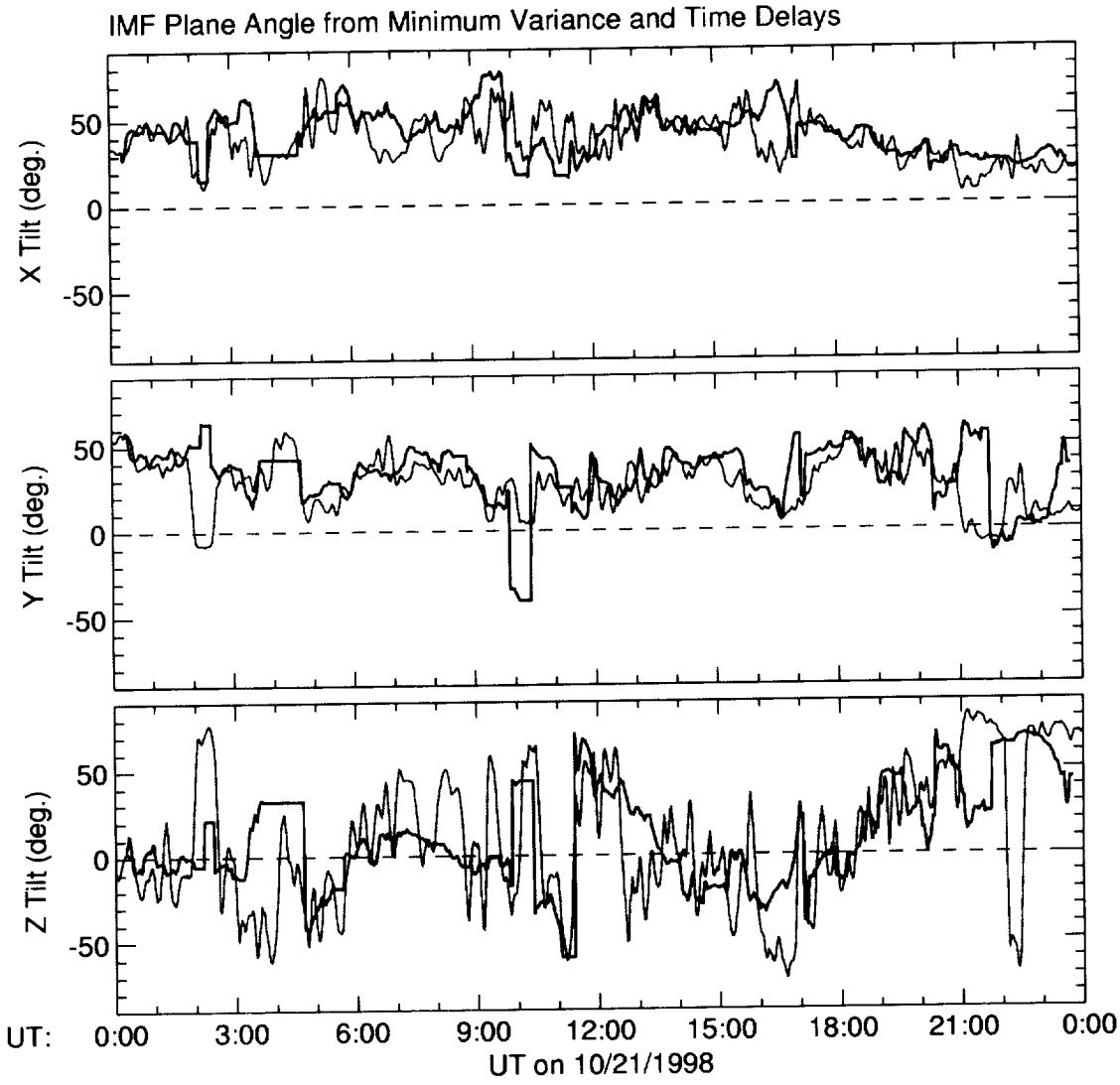

Figure 1. Computed IMF tilt angles as a function of time on October 21, 1998. The lighter gray lines show the results from using the propagation time delays between four satellites, and the dark black lines are the results obtained with the minimum variance method. The graphs show the angle between the tilt plane's normal vector and the three GSE coordinate axes.

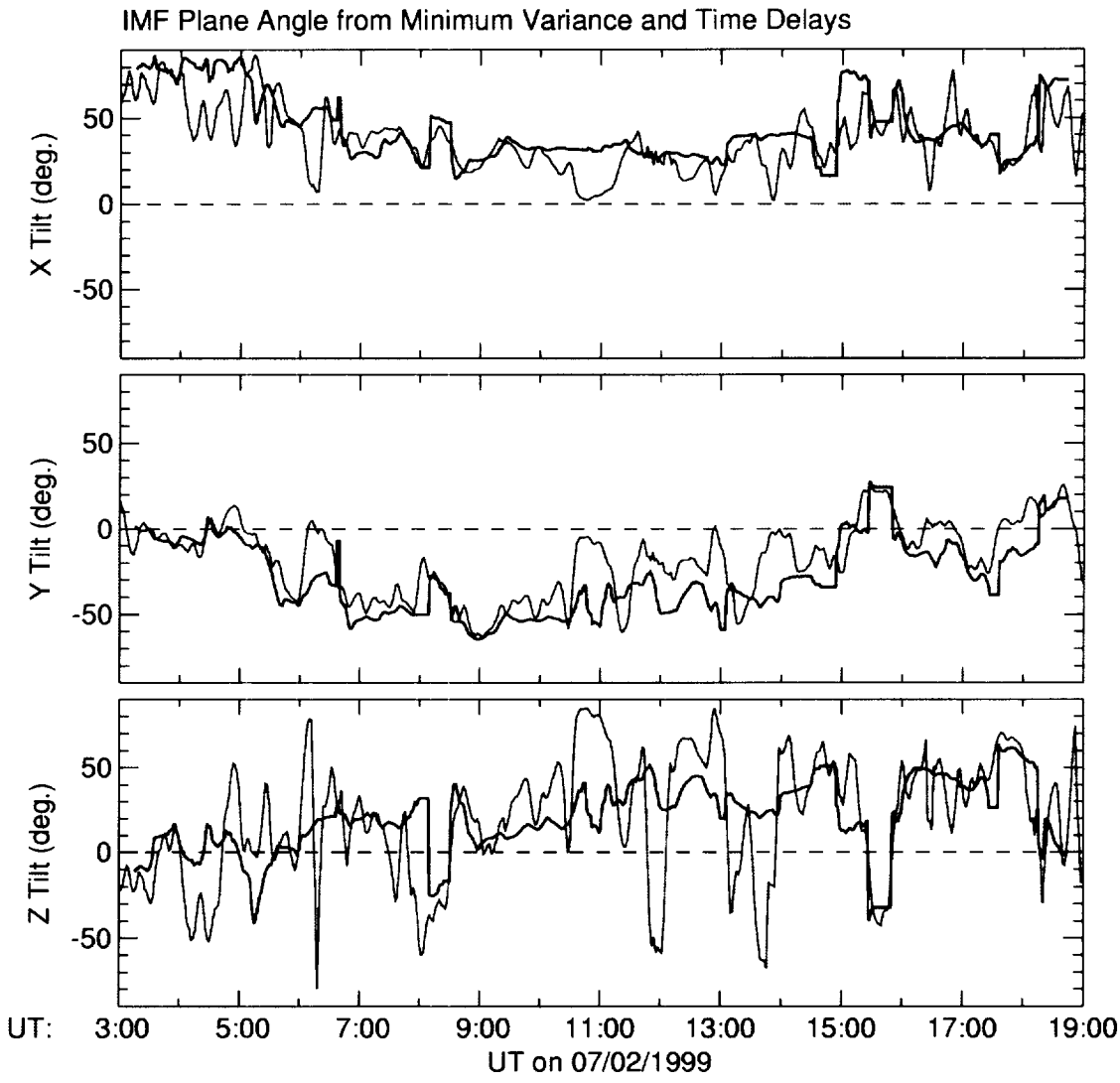

Figure 2. Computed IMF tilt angles as a function of time on July 2, 1999. The format is the same as in Figure 1.

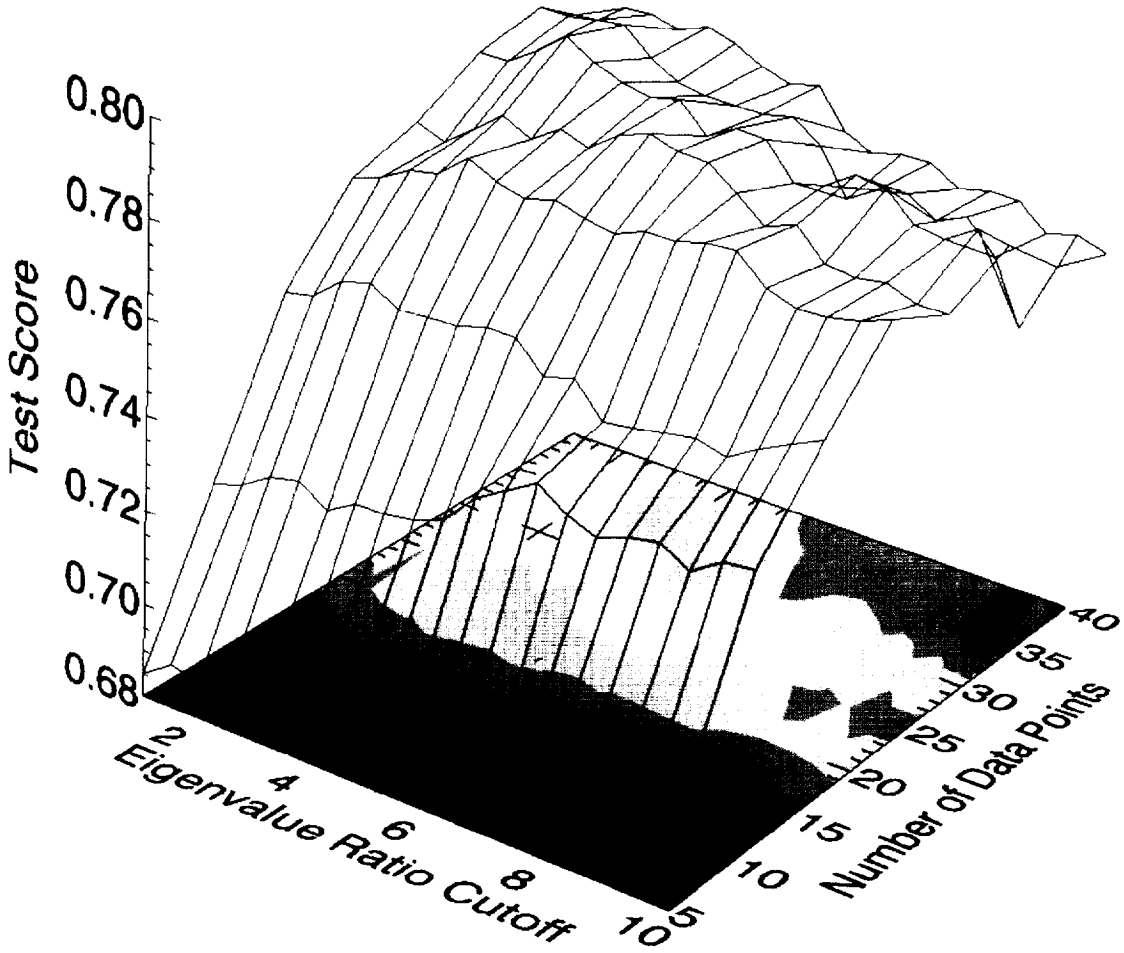

Figure 3. Performance test score of the minimum variance technique as a function of both the number of points used and the eigenvalue ratio cutoff. These scores were obtained by a comparison of the minimum variance results with those from the four-satellite time delay technique. The score is the average dot product from every measurement within four days. Using IMF data from 64 s samples, the best results were found with 30 data points and using 2.5 as the minimum requirement for the eigenvalue ratio.

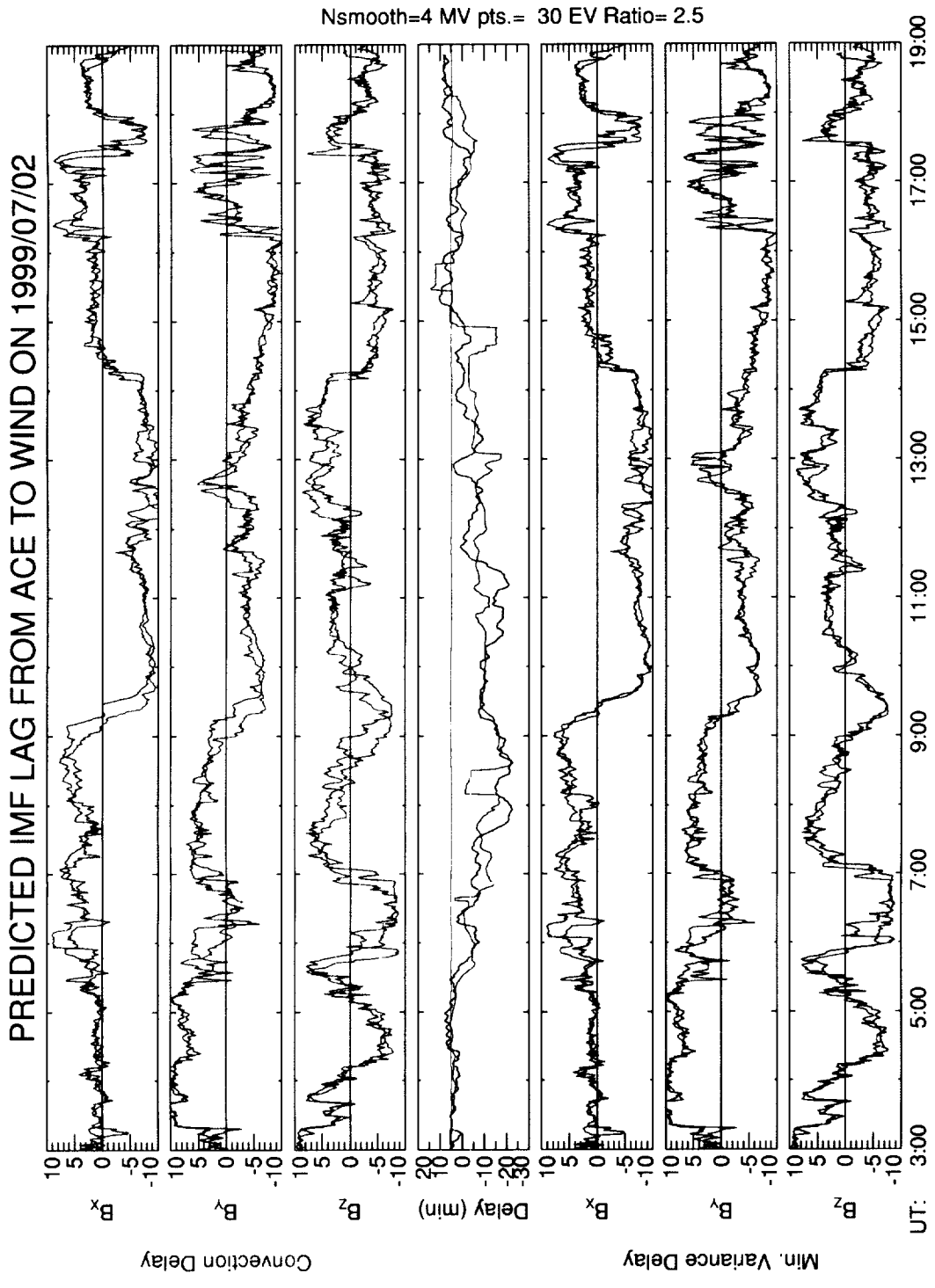

Plate 1. Comparison of the IMF measurements from both the ACE and Wind satellites for the case on July 2, 1999. The top three panels show the three components of the IMF measured at ACE in black, while the green lines show the Wind measurements, after first shifting these data in time according to a flat plane propagation at the solar wind velocity. The delay time that was used is shown as the green line in the middle plot. The bottom three panels show the same ACE data, again in black, but this time the Wind data have been shifted in time according to the tilt angles from the minimum variance technique, as shown in blue. The value of these time shifts are shown as blue in the middle. For comparison, the time delay curve that was found to give the best match between the measurements is shown in red.

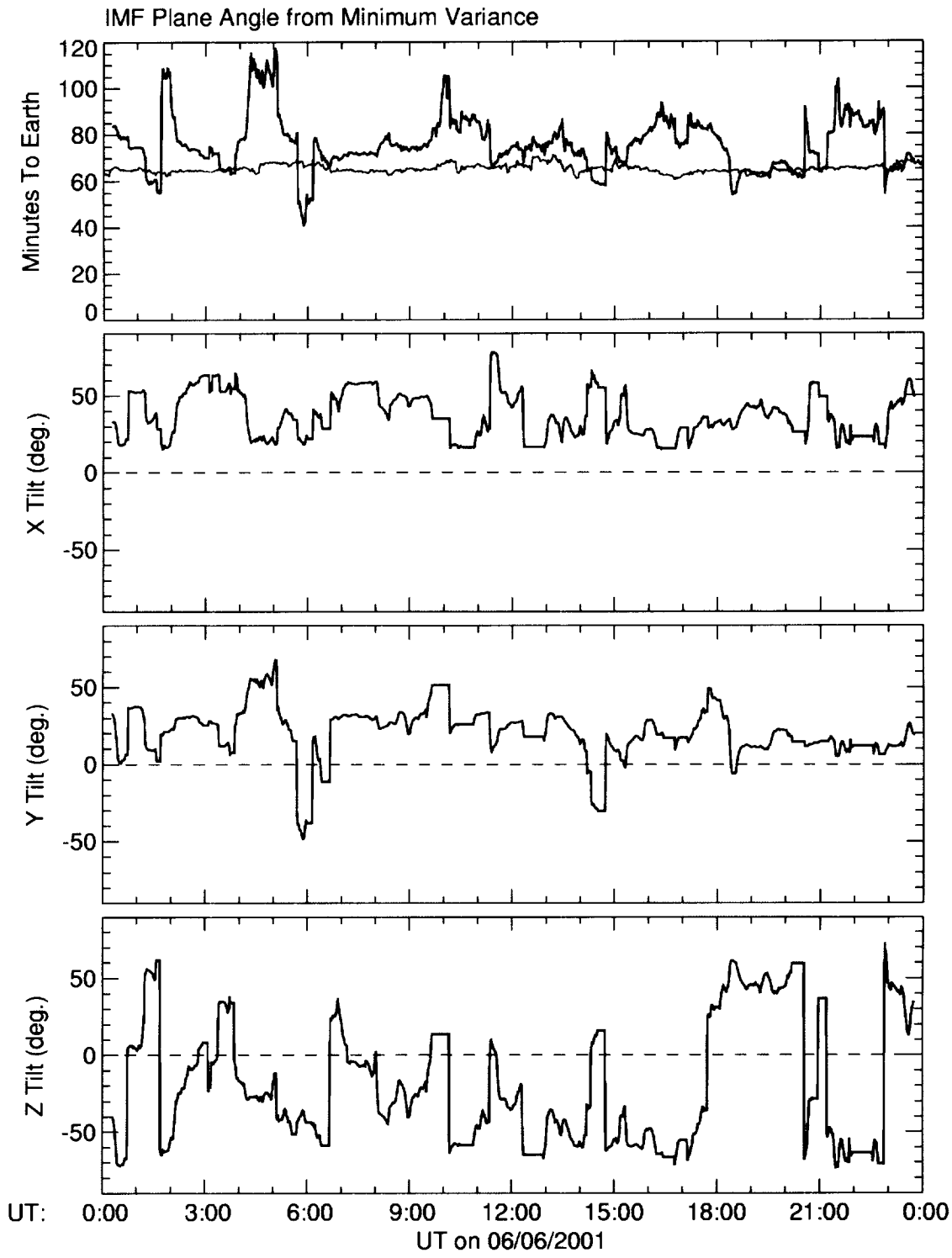

Figure 4. Computed IMF tilt angles as a function of time on June 6, 2001. The format is the same as in Figure 1, only in this case the results are shown from the minimum variance technique only, using measurements from ACE. Additionally, the top panel shows the propagation delay time, from ACE to Earth, that is obtained by using these tilt angles. For comparison, the lighter gray lines show the time delay that is obtained without using any tilt.

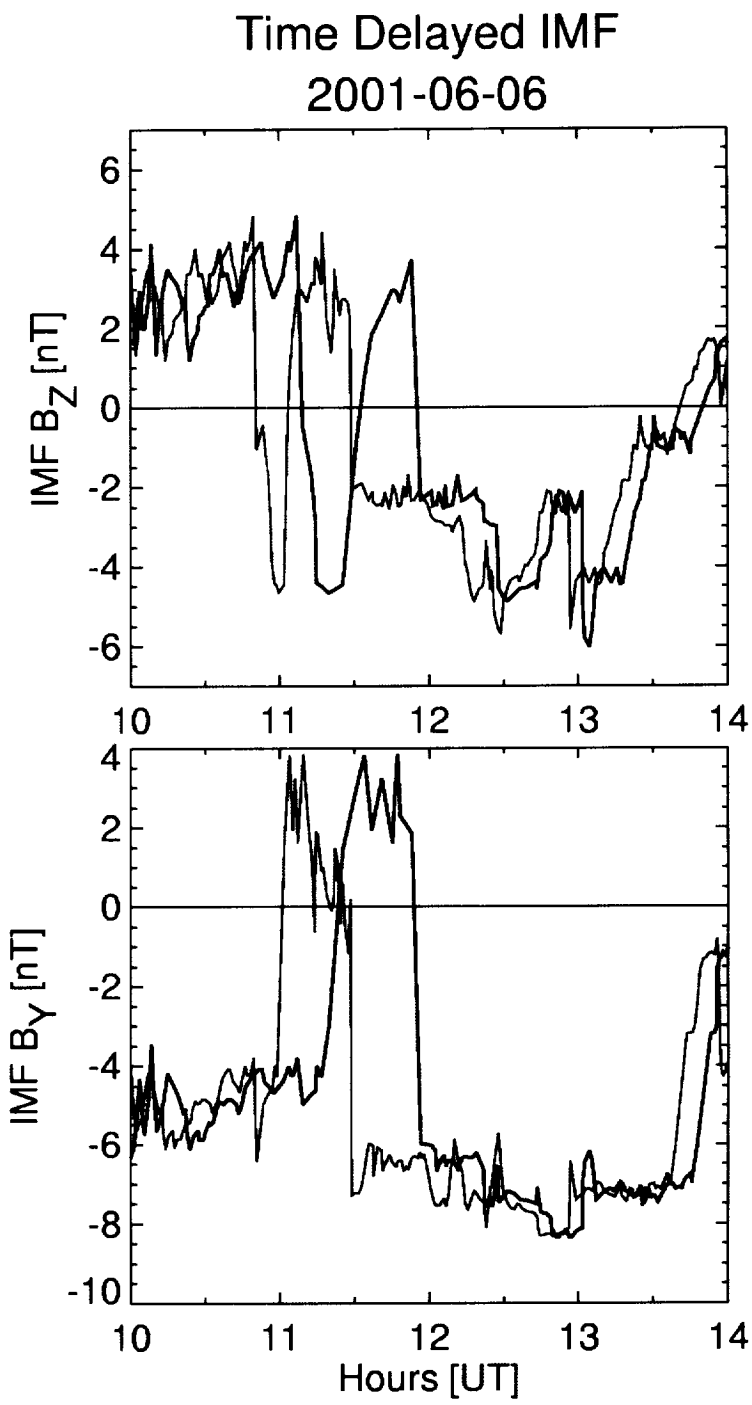

Figure 5. The Y and Z components of the IMF that were measured by ACE on June 6, 2001. These measurements have been shifted in time by using the two different delay values that were plotted in Figure 4, thus giving two different predictions for the IMF variations at the Earth. The darker lines show the results from using the minimum variance calculations.

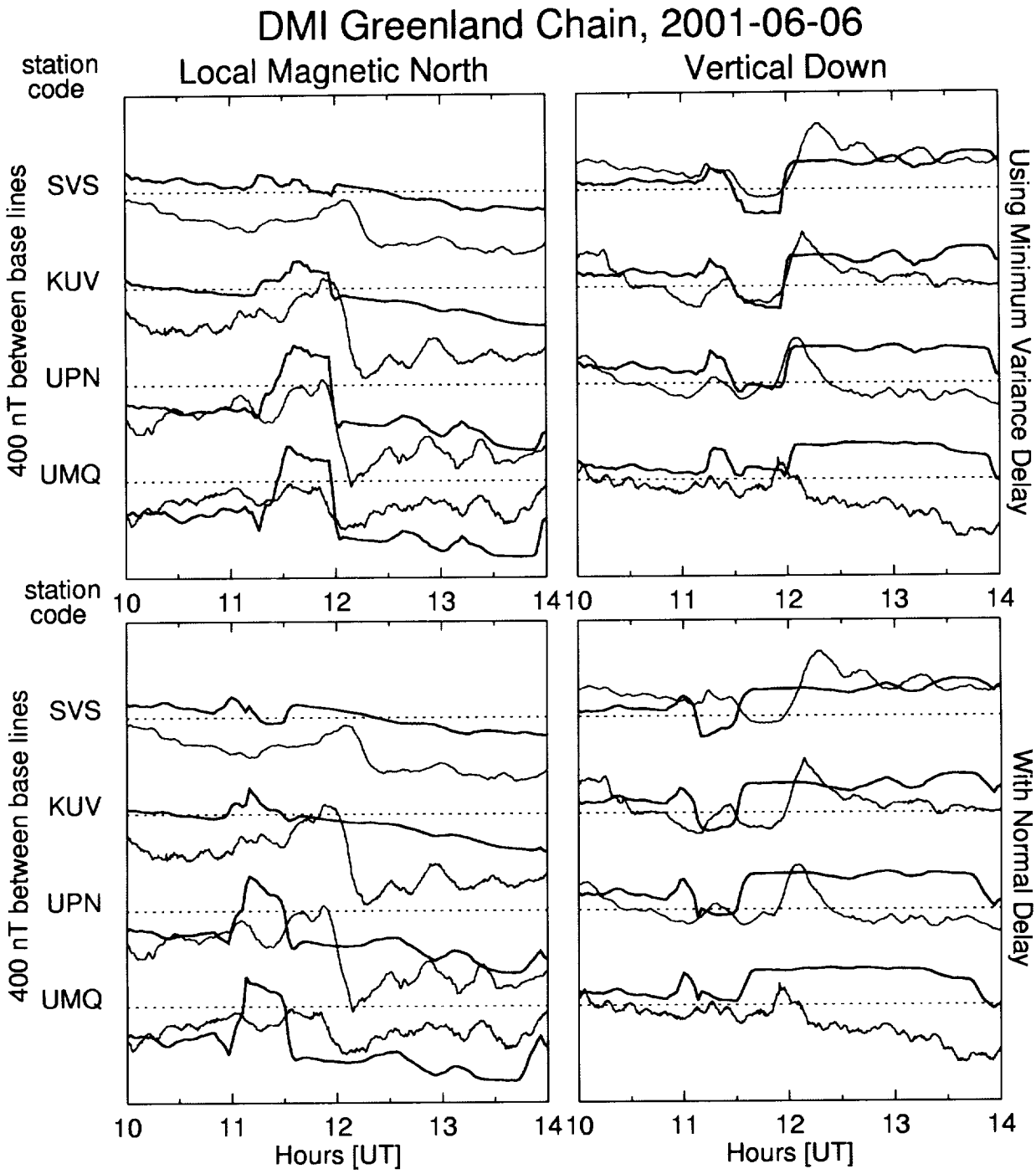

Figure 6. A comparison of measured magnetic perturbations and model predictions for 10 to 14 UT on June 6, 2001. The northern and vertical components of the magnetic perturbations are shown for four northern stations in the Greenland Chain, using the light gray lines. The darker black lines show the results from predicting these variations with a technique that uses the IMF data shown in Figure 5. The upper row uses the IMF that were shifted in time according to the minimum variance tilt angles, while the bottom row uses the flat plane propagation.

REPORT DOCUMENTATION PAGE

Form Approved
OMB No. 0704-0188

1. AGENCY USE ONLY *(Leave blank)*	2. REPORT DATE	3. REPORT TYPE AND DATES COVERED
	14 March 2002	Final, 4 March 1999 - 4 March 2002

4. TITLE AND SUBTITLE
Final Report for NASW-99004

5. FUNDING NUMBERS
C NASW-99004

6. AUTHORS
Daniel R Weimer

7. PERFORMING ORGANIZATION NAME(S) AND ADDRESS(ES)
Mission Research Corporation
735 State St.; PO Drawer 719
Santa Barbara, CA 93102-0719

8. PERFORMING ORGANIZATION REPORT NUMBER
C-44047-Final

9. SPONSORING/MONITORING AGENCY NAME(S) AND ADDRESS(ES)
National Aeronautics and Space Administration
Goddard Space Flight Center, Headquarters Procurement Office
Code 210.H, Greenbelt, MD 20771

10. SPONSORING/MONITORING AGENCY REPORT NUMBER

11. SUPPLEMENTARY NOTES

12a. DISTRIBUTION/AVAILABILITY STATEMENT
unlimited

12b. DISTRIBUTION CODE

13. ABSTRACT *(Maximum 200 words)*

Measurements of the interplanetary magnetic field (IMF) from the ACE, Wind, IMP-8, and Geotail spacecraft have revealed that the IMF variations are contained in phase planes that are tilted with respect to the propagation direction, resulting in continuously variable changes in propagation times between spacecraft, and therefore, to the Earth. Techniques for using "minimum variance analysis" have been developed in order to be able to measure the phase front tilt angles, and better predict the actual propagation times from the L1 orbit to the Earth, using only the real-time IMF measurements from one spacecraft. The use of empirical models with the IMF measurements at L1from ACE (or future satellites) for predicting "space weather" effects has also been demonstrated.

14. SUBJECT TERMS
ionospheric electric fields and currents, solar wind terrestrial energy coupling, interplanetary magnetic field, solar wind

15. NUMBER OF PAGES
35

16. PRICE CODE

17. SECURITY CLASSIFICATION OF REPORT	18. SECURITY CLASSIFICATION OF THIS PAGE	19. SECURITY CLASSIFICATION OF ABSTRACT	20. LIMITATION OF ABSTRACT
UNCLASSIFIED	UNCLASSIFIED	UNCLASSIFIED	UL